Newcastle University

ePrints

Gao Y, Chakraborty N. Modelling of Lewis Number dependence of Scalar dissipation rate transport for Large Eddy Simulations of turbulent premixed combustion. *Numerical Heat Transfer A* 2016, 69(11), 1201-1222.

Copyright:

This is an Open Access article distributed under the terms of the Creative Commons Attribution License (http://creativecommons.org/licenses/by/3.0), which permits unrestricted use, distribution, and reproduction in any medium, provided the original work is properly cited. The moral rights of the named author(s) have been asserted.

DOI link to article:

http://dx.doi.org/10.1080/10407782.2015.1125732

Date deposited:

27/07/2016

This work is licensed under a Creative Commons Attribution 3.0 Unported License

Newcastle University ePrints - eprint.ncl.ac.uk

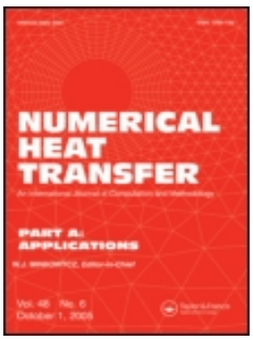

Taylor & Francis
Taylor & Francis Group

Numerical Heat Transfer, Part A: Applications
An International Journal of Computation and Methodology

ISSN: 1040-7782 (Print) 1521-0634 (Online) Journal homepage: http://www.tandfonline.com/loi/unht20

Modeling of Lewis number dependence of scalar dissipation rate transport for Large Eddy Simulations of turbulent premixed combustion

Yuan Gao & Nilanjan Chakraborty

To cite this article: Yuan Gao & Nilanjan Chakraborty (2016) Modeling of Lewis number dependence of scalar dissipation rate transport for Large Eddy Simulations of turbulent premixed combustion, Numerical Heat Transfer, Part A: Applications, 69:11, 1201-1222

To link to this article: http://dx.doi.org/10.1080/10407782.2015.1125732

Published with license by Taylor & Francis©
Yuan Gao and Nilanjan Chakraborty
Published with license by Taylor & Francis

Published online: 02 May 2016.

Submit your article to this journal

Article views: 178

View related articles

View Crossmark data

Full Terms & Conditions of access and use can be found at
http://www.tandfonline.com/action/journalInformation?journalCode=unht20

Download by: [Newcastle University] **Date:** 27 July 2016, At: 06:32

NUMERICAL HEAT TRANSFER, PART A
2016, VOL. 69, NO. 11, 1201–1222
http://dx.doi.org/10.1080/10407782.2015.1125732

Taylor & Francis
Taylor & Francis Group

OPEN ACCESS

Modeling of Lewis number dependence of scalar dissipation rate transport for Large Eddy Simulations of turbulent premixed combustion

Yuan Gao and Nilanjan Chakraborty

School of Mechanical and Systems Engineering, Newcastle University, Newcastle-Upon-Tyne, UK

ABSTRACT

The influences of differential diffusion of heat and mass on the Favre-filtered scalar dissipation rate (SDR) transport have been analyzed and modeled using *a priori* analysis of Direct Numerical Simulations (DNS) data of freely propagating statistically planar turbulent premixed flames with different values of global Lewis number, Le. The DNS data has been explicitly filtered using a Gaussian filter to obtain the unclosed terms of the Favre-filtered SDR transport equation, arising from turbulent transport (T_1), density variation due to heat release (T_2), strain rate contribution due to the alignment of scalar and velocity gradients (T_3), correlation between the gradients of reaction rate and reaction progress variable (T_4), molecular dissipation of SDR ($-D_2$), and diffusivity gradients $f(D)$. The statistical behaviors of these terms and their scaling estimates reported in a recent analysis have been utilized here to propose models for these unclosed terms in the context of Large Eddy Simulations (LES) and the performances of these models have been assessed using the values obtained from explicitly filtered DNS data. These newly proposed models are found to satisfactorily predict both the qualitative and quantitative behaviors of these unclosed terms for a range of filter widths Δ for all Le cases considered here.

ARTICLE HISTORY
Received 7 September 2015
Accepted 15 October 2015

Downloaded by [Newcastle University] at 06:32 27 July 2016

1. Introduction

Lean premixed combustion has been identified as one of the possible ways to reduce pollutant emission from gasoline engines and industrial gas turbines [1]. Lean hydrogen and hydrogen-blended hydrocarbon combustion has the potential to attenuate pollutants and greenhouse gas emissions [2, 3]. However, the flames with abundance of fast diffusing species such as hydrogen either in molecular or in atomic form give rise to a significant level of differential diffusion of heat and mass. The differential diffusion of heat and mass can be characterized by a nondimensional number known as the Lewis number *Le*, which is defined as the ratio of thermal diffusivity α_T to mass diffusivity D (i.e., $Le = \alpha_T/D$). In actual premixed combustion it is often not straightforward to assign a single global Lewis number in the presence of several species with different Lewis numbers. Often the Lewis number of the deficient species is considered to be the global Lewis number [4], whereas Law and Kwon [5] proposed a methodology of evaluating the effective Lewis number based on heat release measurements. More recently Dinkelacker et al. [6] proposed an algebraic expression for the effective Lewis number based on mole fractions of major species. A number of previous analyses concentrated on the effects of global Lewis number on different aspects of premixed combustion in isolation [7–28] and the same approach has been adopted here.

CONTACT Nilanjan Chakraborty nilanjan.chakraborty@ncl.ac.uk School of Mechanical and Systems Engineering, Newcastle University, Claremont Road, Newcastle-Upon-Tyne NE1 7RU, UK.
Color versions of one or more of the figures in the article can be found online at www.tandfonline.com/unht.
This is an Open Access article distributed under the terms of the Creative Commons Attribution License (http://creativecommons.org/licenses/by/3.0), which permits unrestricted use, distribution, and reproduction in any medium, provided the original work is properly cited. The moral rights of the named author(s) have been asserted.
Published with license by Taylor & Francis © Yuan Gao and Nilanjan Chakraborty

Downloaded by [Newcastle University] at 06:32 27 July 2016

Nomenclature

c	reaction progress variable	u_i	i^{th} component of nondimensional fluid velocity
c_m	thermo-chemical parameter		
C_P	specific heat at constant pressure	u'	root mean square fluctuation of velocity
C_V	specific heat at constant volume	u'_Δ	sub-grid velocity fluctuation
C_F	model parameter	$\dot{w}$	chemical reaction rate
C_3, C_4	model parameters	x_i	i^{th} Cartesian coordinate
D	progress variable diffusivity	Y_R	reactant mass fraction
D_t	eddy diffusivity	Y_{R0}	reactant mass fraction in unburned gas
Da	Damköhler number	$Y_{R\infty}$	reactant mass fraction in burned gas
D_1	molecular diffusion term	α_T	thermal diffusivity
D_2	molecular dissipation term	α_{T0}	thermal diffusivity of the unburned gas
f_b	burning mode probability density function	β	Zel'dovich number
		β_3, β'_3	model parameters
f_{T_2}, f_{T_3}, f_{TD}	model parameters	γ	ratio of specific heats ($=C_P/C_V$)
$f(D)$	term due to diffusivity gradient	γ_1, γ_2	model parameter
k_{sgs}	sub-grid scale kinetic energy	δ_{th}	thermal flame thickness
K_c^*	thermo-chemical parameter	δ_z	Zel'dovich flame thickness
Ka	Karlovitz number	Δ	filter width
Le	Lewis number	Γ	model parameter
l	integral length scale	μ	viscosity
Ma	Mach number	μ_0	viscosity of unburned gas
M_i	ith component of resolved flame normal	ρ	density
N_c	scalar dissipation rate	ρ_0	unburned gas density
N_i	ith component of flame normal	τ	heat release parameter
p	model parameter	τ_{ij}	viscous stress tensor
Pr	Prandtl number	Φ'	model parameter
Q	general quantity	$\overline{q}$	LES-filtered value of a general quantity q
Re_t	turbulent Reynolds number	$\tilde{q}$	Favre-filtered value of a general quantity q
Re_Δ	sub-grid Reynolds number		
S_L	unstrained laminar burning velocity	***Subscripts***	
t	time	0	unburned gas value
t_c	chemical time scale	∞	burned gas value
t_f	initial turbulent eddy turnover time	*res*	resolved scale value
t_{sim}	simulation time	*sg*	sub-grid scale value
T	instantaneous dimensional temperature		
T^+	non-dimensional temperature	***Acronyms***	
T_{ad}	adiabatic flame temperature	DNS	direct numerical simulation
T_0	reactant temperature	LES	large eddy simulation
T_1, T_2, T_3, T_4	terms in the transport equation of Favre-filtered scalar dissipation rate	pdf	probability density function
		SDR	scalar dissipation rate

Modeling of the differential diffusion arising from non-unity global Lewis number remains pivotal to high-fidelity engineering simulations, which are likely to play important roles in the development of new-generation combustors using either hydrogen or hydrogen-blended fuels. Prediction of the micro-mixing rate of hot products and cold unburned gas plays a key role in the modeling of turbulent reacting flows and a quantity known as the scalar dissipation rate (SDR) characterizes this micro-mixing rate [29, 30–32]. Furthermore, the Favre-mean value of SDR of reaction progress variable c in premixed turbulent flames can be related to the mean reaction rate in the context of Reynolds Averaged Navier Stokes (RANS) simulations [23, 33–35]. The instantaneous SDR of reaction progress variable is defined as [23, 33–38]

$$N_c = D\nabla c \cdot \nabla c \tag{1}$$

where D is the diffusivity of reaction progress variable c. Recent analyses have demonstrated [36–38] that the SDR-based reaction rate closure for RANS can also be used for the modeling of the filtered reaction rate $\overline{\dot{w}}$ based on the Favre-filtered SDR of a reaction progress variable (i.e., $\tilde{N}_c = \overline{\rho D\nabla c.\nabla c}/\overline{\rho}$) in the

context of Large Eddy Simulation (LES) in the following manner when the filter size Δ remains greater than the thermal flame thickness $\delta_{th} = (T_{ad} - T_0)/Max|\nabla T|_L$ (where T_{ad}, T_0, and T are the adiabatic flame, unburned gas, and instantaneous temperatures, respectively):

$$\overline{\dot{w}} = \frac{2\overline{\rho}\tilde{N}_c}{(2c_m - 1)} \text{ with } c_m = \frac{\int_0^1 [c\dot{w}]_L f_b(c)dc}{\int_0^1 [\dot{w}]_L f_b(c)dc} \quad (2)$$

where ρ is the density and $\tilde{q} = \overline{\rho Q}/\overline{\rho}$ is the Favre-filtered value of a quantity Q with the over-bar indicating an LES filtering operation. In Eq. (2) $f_b(c)$ is the reacting mode probability density function (pdf) of c and the subscript "L" refers to the planar laminar flame conditions. By assuming $f_b(c)$ as a smooth function, regardless of the exact form, the numerical value of $c_m$remains within a range of 0.7–0.9 for typical hydrocarbon–air mixtures [33].

The modeling of SDR not only is useful for the closure of filtered reaction rate but also plays a pivotal role in the closure of micro-mixing rate in the context of pdf methodology [30, 39–41]. For turbulent premixed flames, the Favre-filtered SDR $\tilde{N}_c$ can be modeled either by using an algebraic expression in terms of the resolved quantities or by solving a modeled transport equation. A few recent analyses [36–41] have concentrated on the algebraic closure of SDR for turbulent premixed flames in the context of LES. Algebraic closures are suitable when an equilibrium is maintained between the generation and destruction rates of $\tilde{N}_c$, but this assumption may be rendered invalid under some conditions (e.g., low Damköhler number lean premixed combustion). A number of previous analyses [34, 42–51] concentrated on the modeling of SDR transport in turbulent premixed combustion in the context of RANS simulations. Interested readers are referred to Ref [34]. for a detailed review of the existing modeling methodologies for SDR transport in the context of RANS simulations. Recent advancements in high-performance computing have made LES of industrial flows more affordable than in the past, and LES is more successful in capturing unsteady flow features than RANS. However, relatively limited attention has been given to the investigation of SDR transport in the context of LES [52, 53]. Recently, models for the unclosed terms of the SDR $\tilde{N}_c$ transport equation for unity Lewis number flames in the context of LES have been proposed [53], but the differential diffusion effects due to non-unity *Le* were not addressed. A recent analysis [28] concentrated on the influences of global *Le* on the statistical behaviors of the unclosed terms of the $\tilde{N}_c$ transport equation based on an order-of-magnitude approach, which successfully explained the effects of global *Le* and the filter width Δ dependences of the Favre-filtered SDR $\tilde{N}_c$ and its transport. It has been found that *Le* has significant influences on both the qualitative and quantitative behaviors of the unclosed terms of the SDR $\tilde{N}_c$ transport equation [22, 28]; however, the modeling of *Le* effects on these unclosed terms is yet to be addressed, and the present analysis aims to address this gap in the existing literature. In this respect the main objectives of this paper are:

i. To propose models for the unclosed terms of the SDR transport equation in such a manner that the performances of these models remain satisfactory for a range of Δ and *Le*.
ii. To assess the performances of the newly proposed models with respect to explicitly filtered Direct Numerical Simulation (DNS) data.

These objectives are addressed here by conducting *a priori* analysis using a DNS database of statistically planar turbulent premixed flames with a range of different values of *Le* (i.e., *Le* = 0.34–1.2). The details related to mathematical background and numerical implementation are provided in the next section. This is followed by the presentation of the results and subsequent discussion. The main findings are summarized and conclusions are drawn in the final section of this paper.

2. Mathematical background & numerical implementation

Three-dimensional DNS simulations with detailed chemistry are now possible, but they remain extremely expensive and need several millions of CPU hours [54] for conducting extensive parametric

Downloaded by [Newcastle University] at 06:32 27 July 2016

variations and carrying out explicit filtering of DNS data using a range of filter widths Δ, as has been carried out in the current study. Thus, the chemical mechanism has been simplified here as a single-step Arrhenius-type irreversible chemical reaction. Under this condition the species field is uniquely represented by a reaction progress variable c, which can be defined by using the mass fraction of a suitable reactant Y_R as $c = (Y_{R0} - Y_R)/(Y_{R0} - Y_{R\infty})$, where subscripts 0 and ∞ denote the values in the unburned and burned gases, respectively. The transport equation of c can be used to derive a transport equation of $\tilde{N}_c = \overline{\rho D \nabla c . \nabla c}/\overline{\rho}$, which takes the following form [28, 53]:

$$\frac{\partial(\overline{\rho}\tilde{N}_c)}{\partial t} + \frac{\partial(\overline{\rho}\tilde{u}_i\tilde{N}_c)}{\partial x_i} = \underbrace{\overline{\frac{\partial}{\partial x_i}\left(\rho D \frac{\partial N_c}{\partial x_i}\right)}}_{D_1} + T_1 + T_2 + T_3 + T_4 - D_2 + f(D) \tag{3}$$

where u_i is the *ith* component of the velocity vector. On the left-hand side of Eq. (3) the terms denote the transient effects and resolved advection of $\tilde{N}_c$, respectively. The term D_1 depicts the molecular diffusion of $\tilde{N}_c$, and the terms T_1, T_2, T_3, T_4, $(-D_2)$, and $f(D)$ are all unclosed and expressed as follows:

$$T_1 = -\frac{\partial}{\partial x_j}\left[\overline{\rho u_j N_c} - \overline{\rho}\tilde{u}_j\tilde{N}_c\right] \tag{4i}$$

$$T_2 = -\overline{\frac{2D}{\rho}\left[\dot{w} + \frac{\partial}{\partial x_j}\left(\rho D \frac{\partial c}{\partial x_j}\right)\right]\frac{\partial c}{\partial x_i}\frac{\partial \rho}{\partial x_i}} \tag{4ii}$$

$$T_3 = -\overline{2\rho D \frac{\partial c}{\partial x_i}\frac{\partial u_i}{\partial x_j}\frac{\partial c}{\partial x_j}} \tag{4iii}$$

$$T_4 = \overline{2D \frac{\partial \dot{w}}{\partial x_i}\frac{\partial c}{\partial x_i}} \tag{4iv}$$

$$(-D_2) = -\overline{2\rho D^2 \frac{\partial^2 c}{\partial x_i \partial x_j}\frac{\partial^2 c}{\partial x_i \partial x_j}} \tag{4v}$$

$$\begin{aligned} f(D) = \overline{f_1(D)} = {} & \overline{2D \frac{\partial c}{\partial x_k}\frac{\partial(\rho D)}{\partial x_k}\frac{\partial^2 c}{\partial x_j \partial x_j}} + \overline{2D \frac{\partial c}{\partial x_k}\frac{\partial^2(\rho D)}{\partial x_j \partial x_k}\frac{\partial c}{\partial x_j}} - \overline{\frac{\partial}{\partial x_j}\left(\rho N_c \frac{\partial D}{\partial x_j}\right)} \\ & - \overline{2\rho D \frac{\partial D}{\partial x_j}\frac{\partial}{\partial x_j}\left(\frac{\partial c}{\partial x_k}\frac{\partial c}{\partial x_k}\right)} + \overline{\rho\left(\frac{\partial c}{\partial x_k}\frac{\partial c}{\partial x_k}\right)\left[\frac{\partial D}{\partial t} + u_j \frac{\partial D}{\partial x_j}\right]} \end{aligned} \tag{4vi}$$

where $\dot{w}$ is the reaction rate of c. The term T_1 represents the effects of sub-grid convection, whereas T_2 denotes the effects of density-variation due to heat release. The term T_3 is determined by the alignment of ∇c with local strain rate $e_{ij} = 0.5(\partial u_i/\partial x_j + \partial u_i/\partial x_i)$, and this term is commonly referred to as the scalar-turbulence interaction term. The term T_4 arises due to the correlation between $\nabla \dot{w}$ and ∇c, whereas $(-D_2)$ denotes the molecular dissipation of SDR; these terms will henceforth be referred to as the reaction rate term and the dissipation term, respectively. The term $f(D)$ denotes the effects of D variation. *A priori* DNS modeling of the above-mentioned unclosed terms will be discussed in Section 3 of this paper.

For the present analysis, a DNS database of freely propagating turbulent premixed flames has been considered. The simulation domain is taken to be a cube of $24.1\delta_{th} \times 24.1\delta_{th} \times 24.1\delta_{th}$, which is discretized using a uniform Cartesian grid of $230 \times 230 \times 230$ points, ensuring about 10 grid points are kept within $Min(\delta_L, \delta_{th})$, where $\delta_L = 1/(Max|\nabla c|_L)$ is an alternative flame thickness based on $|\nabla c|$ and the values of δ_L/δ_{th} for cases A–E (with $Le = 0.34$, 0.6, 0.8, 1.0, and 1.2) are provided in Table 1. The initial values of the normalized root-mean-square (rms) value of turbulent velocity u'/S_L, integral length scale to thermal flame thickness ratio l/δ_{th}, Damköhler number $Da = lS_L/u'\delta_{th}$, Karlovitz number $Ka = (u'/S_L)^{3/2}(l/\delta_{th})^{-1/2}$, turbulent Reynolds number $\mathrm{Re}_t = \rho_0 u' l/\mu_0$, and $\tau = (T_{ad} - T_0)/T_0$ are presented in Table 1 along with domain and grid sizes, where ρ_0 and μ_0 are the unburned gas density and viscosity,

Downloaded by [Newcastle University] at 06:32 27 July 2016

Table 1. Initial values of simulation parameters and nondimensional numbers relevant to the DNS database considered for this analysis.

Case	Le	u'/S_L	δ_L/δ_{th}	l/δ_{th}	τ	Re_t	Da	Ka
A	0.34	7.5	2.17	2.45	4.5	47.0	0.33	13.0
B	0.6	7.5	1.40	2.45	4.5	47.0	0.33	13.0
C	0.8	7.5	1.15	2.45	4.5	47.0	0.33	13.0
D	1.0	7.5	1.0	2.45	4.5	47.0	0.33	13.0
E	1.2	7.5	0.90	2.45	4.5	47.0	0.33	13.0

For all cases $\tau = 4.5$; $\beta = 6.0$; $Pr = 0.7$; $Ma = S_L/\sqrt{\gamma RT_0} = 0.014159$.

respectively, and S_L is the unstrained laminar burning velocity. The flamelet assumption is likely to be valid for the values of u'/S_L and l/δ_{th} considered here, and all cases considered here represent the thin reaction zones regime combustion according to the regime diagram by Peters [55].

The simulations have been carried out using a well-known DNS code called SENGA [56]. For all cases the boundary conditions in the mean flame propagation direction are considered to be partially nonreflecting, whereas boundaries in the transverse directions are considered to be periodic. A 10th order central difference scheme is used for spatial differentiation for the internal grid points and the order of differentiation gradually drops to a one-sided second-order scheme at the non-periodic boundaries. A low-storage third-order Runge-Kutta method is used for explicit time advancement for all the governing equations. In all cases flame–turbulence interaction takes place under decaying turbulence, which necessitates the simulation time $t_{sim} \geq \max(t_f, t_c)$, where $t_f = l/u'$ is the initial eddy turnover time and $t_c = \alpha_{T0}/S_L^2$ is the chemical time scale, with α_{T0} being the unburned gas thermal diffusivity. The simulations have been carried out for about $3.34t_f = 3.34l/u'$, which amounts to approximately $1.75\alpha_{T0}/S_L^2$ for all cases considered here. Several studies [12–15, 19, 57–61] with either similar or smaller simulation time have contributed significantly to the fundamental understanding and modeling of turbulent premixed combustion in the past. By the time the statistics were extracted, the value of u'/S_L in the unburned reactants ahead of the flame had decayed by about 50%, whereas the value of l/δ_{th} had increased by about 1.7 times, relative to their initial values. This database has been used in several previous analyses [20–28] and it was shown in Ref [23]. that the volume-integrated burning rate for the $Le = 1.0$ and 1.2 flames reached quasi-steady state by the time statistics were extracted. However, the $Le < 1.0$ flames are thermo-diffusively unstable and thus the volume-integrated burning rate increases with time for these cases [23]. The qualitative nature of the statistics was found to remain unchanged and the scaling estimates presented in the next section remain valid since $t = 2.0\, l/u'$ for all cases considered here.

The unclosed terms of the transport equation of $\tilde{N}_c$ have been evaluated by explicitly filtering DNS data using a standard three-dimensional Gaussian filter [28, 53, 57, 58, 60]: $G(\vec{r}) = (6/\pi\Delta^2)^{3/2} \exp(-6\vec{r}\cdot\vec{r}/\Delta^2)$ and the filtered values of a general quantity Q are given by the following integral: $\overline{Q}(\vec{x}) = \int Q(\vec{x}-\vec{r})G(\vec{r})d\vec{r}$. In the next section, the results will be presented for Δ ranging from $\Delta \approx 0.4\delta_{th}$ to $\Delta \approx 2.8\delta_{th}$. This range of filter widths is comparable to the range of Δ used in several previous *a priori* DNS analyses [57, 58, 60], and addresses a range of different length scales from Δ comparable to $\delta_{th} \approx 1.75\delta_z$ ($\delta_z = \alpha_{T0}/S_L$ is the Zel'dovich flame thickness) up to $2.8\delta_{th} \approx 5.0\delta_z$, where Δ is comparable to the integral length scale.

3. Results and discussion

The distributions of $\tilde{c}$ on $x_1 - x_2$ mid-plane for $\Delta = 0.8\delta_{th}$, $1.6\delta_{th}$, and $2.8\delta_{th}$ at $t = 1.75\, t_c$ for cases A–E are shown in Figure 1, which shows an increase in the extent of flame wrinkling with decreasing Le. The extent of flame wrinkling can be quantified in terms of the normalized turbulent flame surface area A_T/A_L, where the flame surface area is evaluated using the volume integration of the form: $A = \int_V |\nabla c| dV$ with subscripts "T" and "L" denoting the turbulent and laminar flame values, respectively [28]. The values of A_T/A_L and the normalized turbulent burning velocity S_T/S_L (where $S_T = (\rho_0 A_P)^{-1} \int_V \dot{w} dV$) at $1.75t_c = \delta_{th}/S_L$ are listed in Table 2, which demonstrates that both

Downloaded by [Newcastle University] at 06:32 27 July 2016

Downloaded by [Newcastle University] at 06:32 27 July 2016

Table 2. The effects of Lewis number on normalized flame surface area A_T/A_L and normalized turbulent flame speed S_T/S_L when the statistics were extracted (i.e., $t = 1.75\ \alpha_{T0}/S_L^2$).

Case	A_T/A_L	S_T/S_L
A	3.93	13.70
B	2.66	4.58
C	2.11	2.53
D	1.84	1.83
E	1.76	1.50

A_T/A_L and S_T/S_L increase significantly with decreasing Lewis number. The burning rate per unit area in turbulent flames increases (decreases) compared with the corresponding laminar value as a result of negative (positive) Markstein length [7–10] for the $Le < 1$ ($Le > 1$) flames. This, in turn, leads to $S_T/S_L > A_T / A_L$ ($S_T / S_L < A_T / A_L$) in the $Le < 1$ ($Le > 1$) flames (see Table 2). It can be further seen from Figure 1 that the flame brush thickens (i.e., the magnitude of $\nabla\tilde{c}$ decreases) and the extent of flame wrinkling decreases with increasing Δ as a result of the smearing of local information due to the convolution operation associated with LES filtering. As the SDR is related to the reaction rate, and the gradient of the reaction progress variable, the effects of Le on burning rate and Δ dependence of $\nabla\tilde{c}$ are expected to influence the statistical behavior of SDR $\tilde{N}_c$ and its transport. The effects of Le and Δ on the statistical behavior of SDR $\tilde{N}_c$ and its transport have been analyzed elsewhere [28] and the current analysis will only concentrate on the influences of global Lewis number on the modeling of SDR transport.

The normalized mean values of T_1, T_2, T_3, T_4, $(-D_2)$, and $f(D)$ conditional on $\tilde{c}$ for cases A–E are shown in Figure 2 for $\Delta \approx 0.4\delta_{th}$ and $\Delta \approx 2.8\delta_{th}$. Figure 2 shows that T_2 and $(-D_2)$ act as source and sink, respectively, in all cases, which is consistent with previous findings [21, 28]. The contribution of T_4 is positive for a major portion of the flame brush before becoming negative toward the burned gas side for $\Delta \leq \delta_{th}$ (e.g., $\Delta \approx 0.4\delta_{th}$); however, for $\Delta > \delta_{th}$ (e.g., $\Delta \approx 2.8\delta_{th}$) the contribution of T_4 remains a leading-order source throughout the flame brush. The term T_3 assumes positive values toward the unburned gas side of the flame brush before assuming mostly negative values for the major part of the flame brush in cases D and E, whereas T_3 is negative throughout the flame brush in cases A–C for all filter widths. The contribution of $f(D)$ is negative (positive) toward the unburned (burned) gas side of the flame brush for all cases and for all filter widths. The magnitude of T_1 is negligible compared with T_2, T_3, T_4, $(-D_2)$, and $f(D)$ for all Δ in all cases. It can be seen from Figure 2 that the magnitude of all the terms decrease with increasing Le and Δ, which is consistent with previous findings based on DNS data [22, 28]. The observed behaviors of T_1, T_2, T_3, T_4, $(-D_2)$, and $f(D)$ in response to Le and Δ have recently been explained by Gao et al. [28] using a detailed scaling analysis, and the scaling estimates of the filtered SDR and the unclosed terms of the SDR transport equation are provided in Table 3. It is worth noting that m and n in Table 3 are positive numbers with magnitudes greater than unity, and the functions $g(Le)$, $\varphi(Le)$, $\varphi_1(Le)$, and $\Psi(Le)$ increase with decreasing global Lewis number Le. It can be seen from the scaling estimates in Table 3 that the magnitudes of the terms T_1, T_2, T_3, T_4, $(-D_2)$, and $f(D)$ are expected to increase with decreasing filter width and global Lewis number. Interested readers are referred to [28] for further discussion on the derivation of the scaling estimates of T_1, T_2, T_3, T_4, $(-D_2)$, and $f(D)$, and only the modeling of these terms will be discussed in this paper in the following subsections.

3.1. Modeling of the turbulent transport term T_1

Equation (4i) indicates that the turbulent transport term T_1 could be satisfactorily closed if the sub-grid flux of SDR (i.e., $\overline{\rho u_i N_c} - \overline{\rho}\tilde{u}_i\tilde{N}_c$) is properly modeled. The sub-grid flux of SDR ($\overline{\rho u_i N_c} - \overline{\rho}\tilde{u}_i\tilde{N}_c$) is often modeled using a gradient hypothesis as follows [34]:

$$\left(\overline{\rho u_i N_c} - \overline{\rho}\tilde{u}_i\tilde{N}_c\right) = -\overline{\rho} D_t \frac{\partial \tilde{N}_c}{\partial x_i} \tag{5i}$$

Downloaded by [Newcastle University] at 06:32 27 July 2016

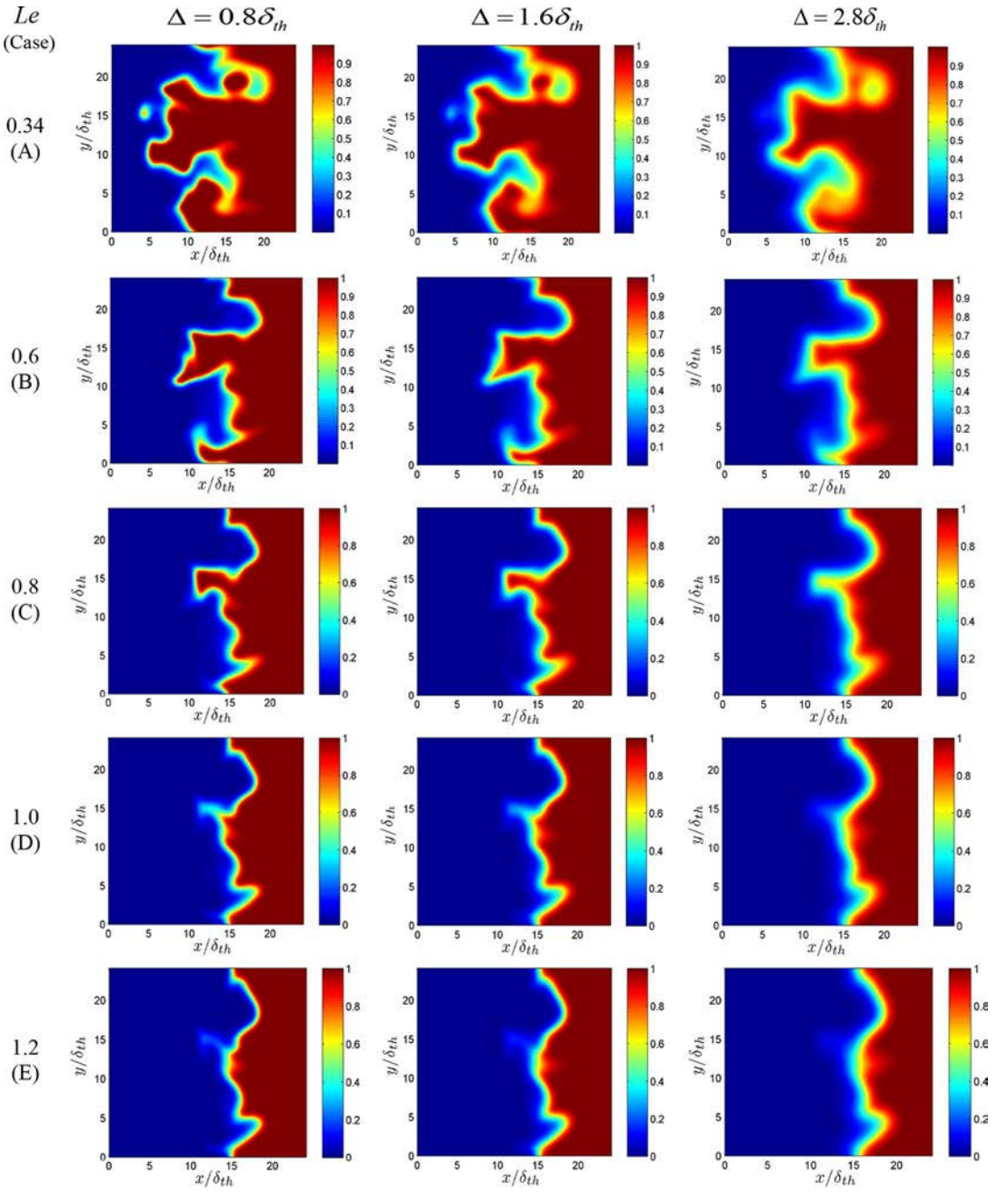

Figure 1. Distributions of $\tilde{c}$ on $x_1 - x_2$ mid-plane for $\Delta = 0.8\delta_{th}$ (1st column), $1.6\delta_{th}$ (2nd column), $2.8\delta_{th}$ (3rd column) for cases A–E (1st–5th row) when the statistics were extracted (i.e., $t = 1.75\ \alpha_{T0}/S_L^2$).

where D_t is the sub-grid scale eddy diffusivity. It has been demonstrated earlier that the turbulent scalar flux of scalar gradients (e.g., flame surface density and SDR) may exhibit counter-gradient (gradient) transport for the flames when counter-gradient (gradient) transport is observed for $(\overline{\rho u_i c} - \overline{\rho}\tilde{u}_i\tilde{c})$ [20, 22, 23, 62]. Thus, the modeling of T_1 needs to include both gradient and counter-gradient transports of $(\overline{\rho u_i N_c} - \overline{\rho}\tilde{u}_i\tilde{N}_c)$.

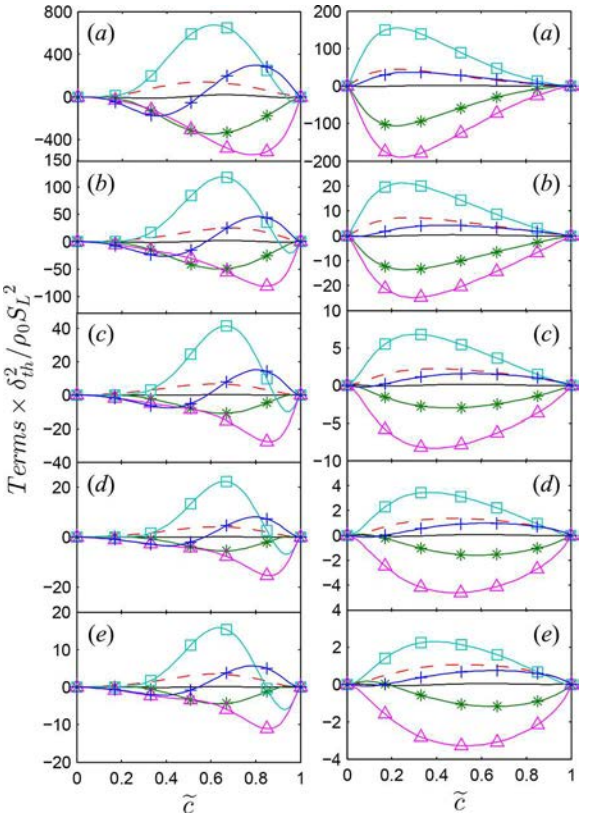

Figure 2. Variations of T_1 (——), T_2 (- - - -), T_3 (—✳—), T_4 (—□—), $(-D_2)$ (—△—), and $f(D)$ (—+—) conditionally averaged in bins of $\tilde{c}$ for $\Delta \approx 0.4\delta_{th}$ (1st column), $1.6\delta_{th}$ (2nd column), and $2.8\delta_{th}$ (3rd column) in cases A–E (1st–5th row). All the terms are normalized with respect to $\rho_0 S_L^2/\delta_{th}^2$.

Table 3. Summary of the scaling estimates of the relevant quantities according to Gao et al. [28].

Quantities	Scaling estimates
$\tilde{N}_c$	$\frac{S_L}{\delta_L}$
$\tilde{D}\nabla\tilde{c}.\nabla\tilde{c}$	$\frac{S_L}{\delta_L} Le^{-2}\mathrm{Re}_\Delta^{-1} Da_\Delta^{-1}$
T_1	$\frac{\tau g_2(Le)\rho_0 S_L^2}{\delta_{th}^2} \times Le \times Da_\Delta^{-0.5}\mathrm{Re}_\Delta^{-0.5}$ alternatively $\frac{\rho_0 S_L^2}{\delta_{th}^2} \times Le \times Da_\Delta^{-1}$
	The above expressions can be combined as $\frac{\overline{(\rho u_i c - \bar{\rho}\tilde{u}_i\tilde{c})}\tilde{N}_c}{\Delta}$
T_2	$\frac{\tau\rho_0 S_L^2}{Le^{m-1}\delta_{th}^2}$
$(T_2)_{res}$ (see Eq. 7ii)	$\frac{\rho_0 S_L^2}{\delta_{th}^2} \times \frac{U_{ref}}{S_L} \times Le^{-1} Re_\Delta^{-1.5} Da_\Delta^{-1.5}$
T_3	$\frac{\tau\rho_0 S_L^2}{Le^{n-1}\delta_{th}^2}$ alternatively $\frac{\rho_0 S_L^2}{\delta_{th}^2} \times Le \times \mathrm{Pr}^{-1/2} \times Ka_\Delta$
$(T_3)_{res}$ (see Eq. 11iii)	$\frac{\rho_0 S_L^2}{\delta_{th}^2} \times \frac{U_{ref}}{S_L} \times Le^{-1} Re_\Delta^{-1.5} Da_\Delta^{-1.5}$
T_4	$\frac{\phi(Le)\rho_0 S_L^2}{\delta_{th}^2}$
$(T_4)_{res}$ (see Eq. 14i)	$\frac{\phi_1(Le)\rho_0 S_L^2}{\delta_{th}^2} \times Re_\Delta^{-1} Da_\Delta^{-1} Le^{-1}$
$(-D_2)$	$\frac{\rho_0\Psi(Le)^2 S_L^2}{\delta_{th}^2} \times Le^{-2}$ alternatively $(-D_2) \sim \frac{\rho_0 S_L^2}{\delta_{th}^2} \times \frac{Ka_\Delta^2}{Pr^3 Le^2}$
$(-D_2)_{res}$ (see Eq. 14ii)	$\frac{\rho_0 S_L^2}{\delta_{th}^2} \times Le^{-2} Re_\Delta^{-2} Da_\Delta^{-2}$
$f(D)$	$\frac{\rho_0\tau S_L^2}{Le^{m-1}\delta_{th}^2}$
$\{f(D)\}_{res}$ (see Eq. 14iii)	$\frac{\rho_0 S_L^2}{\delta_{th}^2} \times Le^{-2}\mathrm{Re}_\Delta^{-2} Da_\Delta^{-2}$

Downloaded by [Newcastle University] at 06:32 27 July 2016

Gao et al. [28] demonstrated that the unclosed term T_1 can be scaled in the following manner:

$$T_1 \sim \frac{\rho_0 \tau g(Le) S_L \widetilde{N}_c}{\Delta} \sim \frac{\rho_0 \tau g(Le) S_L^2}{\delta_{th}^2} \times Le \times Da_\Delta^{-0.5} \mathrm{Re}_\Delta^{-0.5} \text{ for } \Delta \gg \delta_{th} \tag{5ii}$$

where $g(Le)$ is a function increasing with decreasing Le, which accounts for flame normal acceleration, S_L is used to scale the sub-grid velocity fluctuations associated with sub-grid scalar gradients, and the sub-grid fluctuations of SDR are taken to scale with S_L/δ_L [28]. In Eq. (5ii), $Da_\Delta = \Delta S_L / u'_\Delta \delta_{th}$ and $\mathrm{Re}_\Delta = \rho_0 u'_\Delta \Delta / \mu_0$ are the sub-grid Damköhler number and sub-grid turbulent Reynolds number, respectively, with $u'_\Delta = \sqrt{2k_{sgs}/3}$ and $k_{sgs} = (\overline{\rho u_i u_i} - \overline{\rho}\tilde{u}_i\tilde{u}_i)/2\overline{\rho}$ being the sub-grid turbulent velocity fluctuation and sub-grid kinetic energy, respectively. One obtains $Da_\Delta \mathrm{Re}_\Delta \sim (\Delta/\delta_{th})^2$ using $\mu_0 \sim \rho_0 S_L \delta_{th}$, which indicates that $Da_\Delta \mathrm{Re}_\Delta$ increases with increasing Δ. Alternatively, one obtains the following expression when the sub-grid velocity fluctuations are taken to scale with u'_Δ [28]:

$$T_1 \sim \frac{\rho_0 u'_\Delta \widetilde{N}_c}{\Delta} \frac{\rho_0 S_L^2}{\delta_{th}^2} \times Le \times Da_\Delta^{-1} \text{ for } \Delta \gg \delta_{th} \tag{5iii}$$

It is worth noting that the scaling estimate given by Eq. (5ii) (Eq. (5iii)) is more appropriate for counter-gradient (gradient) transport. Equations (5ii) and (5iii) can be combined to obtain the following scaling estimate, which is valid for both gradient and counter-gradient transport [28]:

$$T_1 \sim \frac{\overline{(\rho u_i N_c} - \overline{\rho}\tilde{u}_i\tilde{N}_c)}{\Delta} \sim \frac{\overline{(\rho u_i c} - \overline{\rho}\tilde{u}_i\tilde{c})\tilde{N}_c}{\Delta} \text{ and } \overline{(\rho u_i N_c} - \overline{\rho}\tilde{u}_i\tilde{N}_c) \sim \overline{(\rho u_i c} - \overline{\rho}\tilde{u}_i\tilde{c})\tilde{N}_c \text{ for } \Delta \gg \delta_{th} \tag{5iv}$$

Gao et al. [53] have recently extended a RANS model proposed by Chakraborty and Swaminathan [51] for the purpose of modeling $\overline{(\rho u_i N_c} - \overline{\rho}\tilde{u}_i\tilde{N}_c)$ for the unity Lewis number flames in the context of LES in the following manner:

$$\overline{\rho u_i N_c} - \overline{\rho}\tilde{u}_i\tilde{N}_c = \left\{ (\Phi' - \tilde{c}) \frac{\gamma_1 [\overline{\rho u_i c} - \overline{\rho}\tilde{u}_i\tilde{c}] - \gamma_2 \overline{\rho}\tilde{c}(1-\tilde{c}) u'_\Delta M_i}{\tilde{c}(1-\tilde{c})} \tilde{N}_c - \overline{\rho}(C_F \Delta) u'_\Delta \frac{\partial \tilde{N}_c}{\partial x_i} \right\} \tag{6i}$$

where $M_i = -(\partial\tilde{c}/\partial x_i)/|\nabla\tilde{c}|$ is the *ith* component of the resolved flame normal vector for LES, $\Phi' = 0.7$ is a model parameter, and the following values have been suggested for γ_1, γ_2, and C_F [53]:

$$\gamma_1 = 1.8, \quad \gamma_2 = 4.9 - 3.2 erf(0.15\mathrm{Re}_\Delta) \text{ and } C_F = 0.11 \tag{6ii}$$

The parameterization given by Eq. (6ii) ensures that γ_2 assumes an asymptotic value for large values of Re_Δ (i.e., $\mathrm{Re}_\Delta \to \infty$). In Eq. (6i), the first term on the right-hand side principally accounts for the effects of flame normal acceleration due to heat release, whereas the last term on the right-hand side of Eq. (6i) represents turbulent transport according to conventional gradient hypothesis. Moreover, the first and second terms on the right-hand side of Eq. (6i) are consistent with the scaling estimates given by Eqs. (5iv) and (5iii), respectively.

The predictions of $J_{sg}^+ = (\overline{\rho u_i N_c} - \overline{\rho}\tilde{u}_i\tilde{N}_c) M_i \times \delta_{th}/\rho_0 S_L^2$ according to Eq. (6i) with $\Phi' = 0.7$ are compared to the corresponding quantity extracted from DNS data for $\Delta \approx 0.4\delta_{th}$, $1.6\delta_{th}$, and $2.8\delta_{th}$ in Figure 3 for cases A–E. Figure 3 shows that even though Eq. (6i) predicts J_{sg}^+ in a reasonable manner in the cases with $Le \approx 1.0$ (e.g., cases C–E), this model does not adequately capture the correct qualitative and quantitative behaviors of J_{sg}^+ for the flames with $Le \ll 1.0$ (i.e., cases A and B). The model given by Eqs. (6i) and (6ii) does not explicitly account for non-unity Lewis number effects, so it is not surprising that this model does not adequately capture the behavior of $(\overline{\rho u_i N_c} - \overline{\rho}\tilde{u}_i\tilde{N}_c)$ for $Le \ll 1.0$ flames where the nondimensional temperature $T^+ = (T - T_0)/(T_{ad} - T_0)$ is significantly different from the reaction progress variable c, which alters the distribution of heat release and

Downloaded by [Newcastle University] at 06:32 27 July 2016

Downloaded by [Newcastle University] at 06:32 27 July 2016

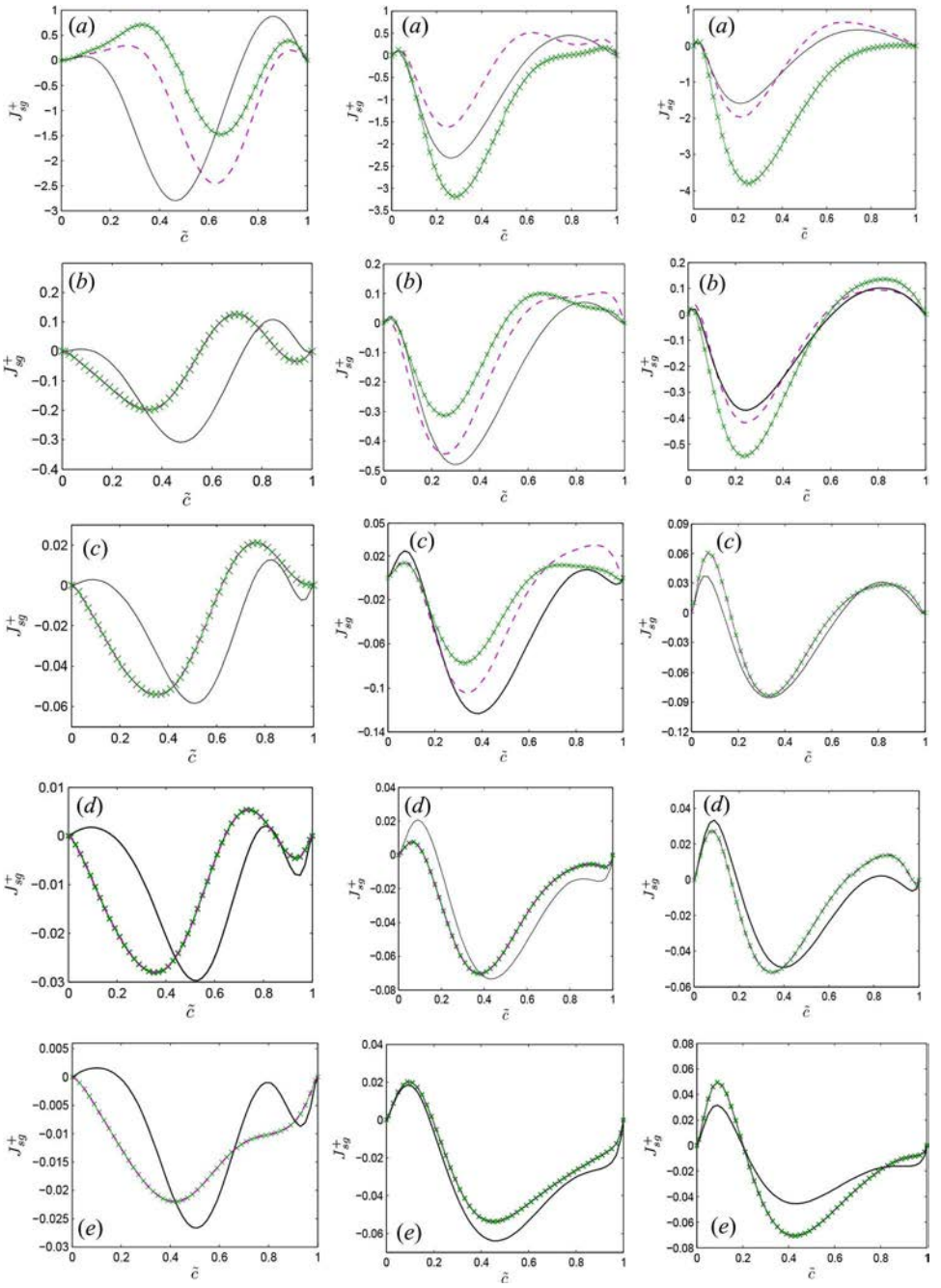

Figure 3. Variations of $J_{sg}^{+} = (\overline{\rho u_i N_c} - \overline{\rho}\tilde{u}_i\tilde{N}_c)M_i \times \delta_{th}/\rho_0 S_L^2$ (——) conditionally averaged in bins of $\tilde{c}$ along with the predictions of Eqs. (6i) and (6ii) with $\Phi' = 0.7$ (—×—) and Eqs. (6i) and (6ii) with Φ' according to Eq. (6iii) (– – –) for $\Delta \approx 0.4\delta_{th}$ (1st column), $1.6\delta_{th}$ (2nd column), and $2.8\delta_{th}$ (3rd column) in cases A–E (1st–5th row).

thermal expansion within the flame brush compared with the $Le \approx 1.0$ flames. This behavior is mimicked here by introducing Le dependence of the model parameter Φ' in the following manner:

$$\Phi' = 0.3(1 - Le) + 0.7 \tag{6iii}$$

Downloaded by [Newcastle University] at 06:32 27 July 2016

The predictions of the model given by Eq. (6i) with Φ' according to Eq. (6iii) are also shown in Figure 3, which demonstrates that the model with new parameterization $\Phi' = 0.3(1 - Le) + 0.7$ predicts J_{sg}^{+} satisfactorily for all filter widths in all cases considered here and the agreement between the predictions of Eq. (6i) and DNS data improves with increasing Δ (see Figure 3). The predictions of Eq. (6i) with Φ' according to Eq. (6iii) become equal to the corresponding values obtained for $\Phi' = 0.7$ for the $Le = 1.0$ case, and these two predictions cannot be distinguished from each other for case D in Figure 3. It worth noting that the sub-grid flux of the reaction progress variable (i.e., $\overline{\rho u_i c} - \overline{\rho}\tilde{u}_i\tilde{c}$) requires modeling in LES, and the performances of the models for $(\overline{\rho u_i N_c} - \overline{\rho}\tilde{u}_i\tilde{N}_c)$ and the turbulent transport term T_1 depend on the modeling of $(\overline{\rho u_i c} - \overline{\rho}\tilde{u}_i\tilde{c})$. The modeling of $(\overline{\rho u_i c} - \overline{\rho}\tilde{u}_i\tilde{c})$ is beyond the scope of the current analysis and interested readers are referred to recent investigations by Chakraborty and Cant [63] and Gao et al. [64] for further discussion on the modeling of turbulent scalar fluxes in premixed turbulent flames.

3.2. Modeling of the density variation term T_2

For unity Lewis number flames the gas density ρ can be expressed as $\rho_0/(1 + \tau c)$ [33], which leads to an alternative expression for the density variation term T_2 as [22, 47, 48, 51, 53]: $T_2 = 2\overline{(\rho\nabla \cdot \vec{u}N_c)}$. However, $\rho = \rho_0/(1 + \tau T^{+}) \neq \rho_0/(1 + \tau c)$ in the non-unity Lewis number flames because the equality between T^{+} and c no longer holds. Although $T_2 = 2\overline{(\rho\nabla \cdot \vec{u}N_c)}$ does not strictly hold in non-unity Lewis number flames, the gas density can still be scaled as $\rho \sim \rho_0/(1 + \tau c)$; thus, the density variation term T_2 can be scaled for adiabatic flames with low Mach number as follows [28]:

$$T_2 \sim 2\overline{\left(\rho\frac{\partial u_i}{\partial x_i}N_c\right)} \sim \frac{\rho_0\tau S_L^2}{Le^{m-1}\delta_{th}^2} \tag{7i}$$

where m is a positive number greater than unity (i.e., $m > 1$). The resolved part of T_2 can be taken to scale as [28]

$$\begin{aligned}(T_2)_{res} &= -\frac{2\tilde{D}}{\overline{\rho}}\left[\dot{\overline{w}} + \frac{\partial}{\partial x_j}\overline{\left(\rho D\frac{\partial c}{\partial x_j}\right)} - \frac{\partial[\overline{\rho u_j c} - \overline{\rho}\tilde{u}_j\tilde{c}]}{\partial x_j}\right]\frac{\partial\tilde{c}}{\partial x_i}\frac{\partial\overline{\rho}}{\partial x_i} \\ &\sim 2\overline{\rho}\tilde{D}\nabla\tilde{c}.\nabla\tilde{c}\frac{\partial\tilde{u}_i}{\partial x_i} \sim \frac{\rho_0 S_L^2}{\delta_{th}^2} \times \frac{U_{ref}}{S_L} \times Le^{-1}Re_{\Delta}^{-1.5}Da_{\Delta}^{-1.5}\end{aligned} \tag{7ii}$$

where U_{ref} is a velocity scale representing the Favre-filtered velocity components $\tilde{u}_i$. It is worth noting that $\overline{\rho} = \rho_0/(1 + \tau\tilde{c})$ for unity Lewis number flames yields $(T_2)_{res} = 2\overline{\rho}\tilde{D}\nabla\tilde{c}\,.\,\nabla\tilde{c}(\partial\tilde{u}_i/\partial x_i)$; however, the expression $\overline{\rho} = \rho_0/(1 + \tau\tilde{c})$ does not strictly hold for non-unity Lewis number flames, but $\overline{\rho}$ and $(T_2)_{res}$ can still be scaled using $\rho_0/(1 + \tau\tilde{c})$ and $2\overline{\rho}\tilde{D}\nabla\tilde{c}\,.\,\nabla\tilde{c}(\partial\tilde{u}_i/\partial x_i)$, respectively.

The scaling estimates given by Eqs. (7i) and (7ii) demonstrate that T_2 remains of the order of $\rho_0\tau S_L^2/\delta_{th}^2$ irrespective of Δ. By contrast, the magnitude of $(T_2)_{res}$ remains comparable to $\rho_0 S_L^2/\delta_{th}^2$ for $U_{ref} \sim S_L$ and $\Delta \approx \delta_{th}$; however, the magnitude of $(T_2)_{res}$ is expected to decrease with increasing Δ. This suggests that the sub-grid component $(T_2)_{sg} = T_2 - (T_2)_{res}$ plays an increasingly important role with increasing Δ, which can be substantiated from Figure 4, where the variations of the mean values of T_2 and $(T_2)_{sg} = T_2 - (T_2)_{res}$ conditional on $\tilde{c}$ are shown for cases A–E for $\Delta \approx 0.4\delta_{th}$, $1.6\delta_{th}$, and $2.8\delta_{th}$.

Gao et al. [53] recently proposed the following model T_2 for unity Le flames in the following manner:

$$T_2 = \underbrace{-\frac{2\tilde{D}}{\overline{\rho}}\left[\dot{\overline{w}} + \frac{\partial}{\partial x_j}\overline{\left(\rho D\frac{\partial c}{\partial x_j}\right)} - \frac{\partial[\overline{\rho u_j c} - \overline{\rho}\tilde{u}_j\tilde{c}]}{\partial x_j}\right]\frac{\partial\tilde{c}}{\partial x_i}\frac{\partial\overline{\rho}}{\partial x_i}}_{(T_2)_{res}} + \beta_{T_2}\tau S_L\frac{[\overline{\rho}\tilde{N}_c - \overline{\rho}\tilde{D}\nabla\tilde{c}.\nabla\tilde{c}]}{\delta_{th}(1.0 + Ka_{\Delta})^{1/2}} \tag{8}$$

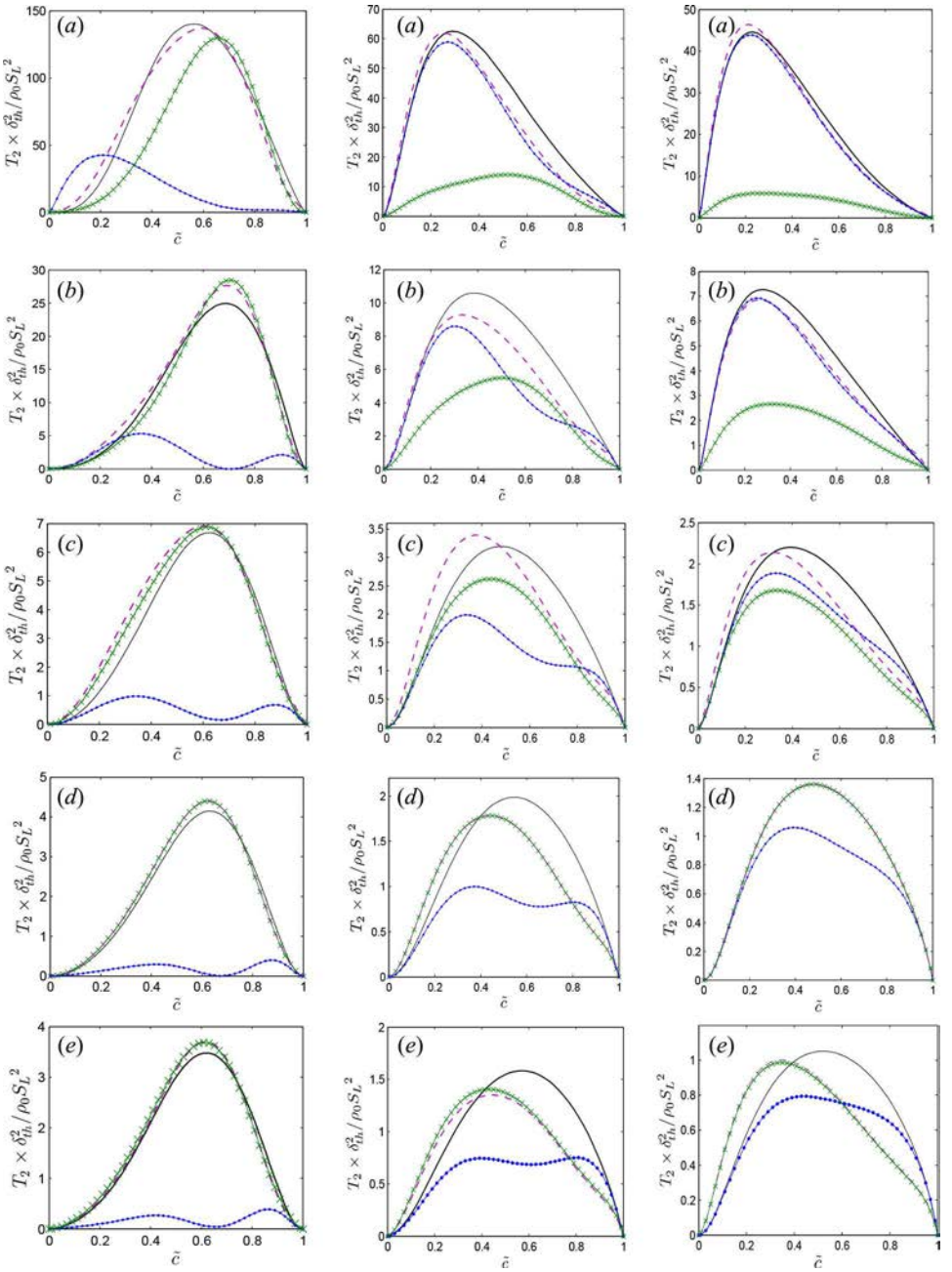

Figure 4. Variations of T_2 (——) and $(T_2)_{sg}$ (——●——) conditionally averaged in bins of $\tilde{c}$ along with the predictions of Eqs. (8) (——×——) and (9) (– – – –) for $\Delta \approx 0.4\delta_{th}$ (1st column), $1.6\delta_{th}$ (2nd column), and $2.8\delta_{th}$ (3rd column) in cases A–E (1st–5th row). All the terms are normalized with respect to $\rho_0 S_L^2/\delta_{th}^2$.

where $Ka_\Delta = (u'_\Delta/S_L)^{3/2}(\Delta/\delta_{th})^{-1/2}$ is local sub-grid Karlovitz number and $\beta_{T_2} = 2.7$ is a model parameter. The first term on the right-hand side of Eq. (8) accounts for the resolved component $(T_2)_{res}$, whereas the second term models the sub-grid component. The Karlovitz number dependence in Eq. (8) ensures the diminishing strength of heat release with increasing Ka_Δ [22, 28, 47, 48, 51, 52] as the combustion process is likely to show the attributes of the broken reaction zones regime [55] (where the effects of heat release are weak) for high values of Karlovitz number. The prediction of

Downloaded by [Newcastle University] at 06:32 27 July 2016

Eq. (8) is also shown in Figure 4 for cases A–E for $\Delta \approx 0.4\delta_{th}$, $1.6\delta_{th}$, and $2.8\delta_{th}$. A comparison between the predictions of Eq. (8) and the normalized T_2 extracted from explicitly filtered DNS data reveals that Eq. (8) satisfactorily predicts T_2 for a range of different filter widths for flames with $Le \approx 1.0$ (e.g., cases C–E); however, this model significantly underpredicts the magnitude of T_2 for the $Le \ll 1.0$ cases (e.g., cases A and B). It can be seen from Eq. (7i) that the magnitude of T_2 is expected to increase with decreasing Le due to the strengthening of heat release effects as a result of the enhanced burning rate for the small values of Lewis number (see Table 2). As this effect is missing in Eq. (8), this model underpredicts the magnitude of T_2 for the $Le \ll 1.0$ cases (e.g., cases A and B), where the effects of enhanced heat release due to the differential diffusion of heat and mass are particularly strong.

Here the model given by Eq. (8) has been extended in order to account for the effects of Le in the following manner:

$$T_2 = \underbrace{-\frac{2\tilde{D}}{\overline{\rho}}\left[\dot{\overline{w}} + \frac{\partial}{\partial x_j}\overline{\left(\rho D\frac{\partial c}{\partial x_j}\right)} - \frac{\partial[\overline{\rho u_j c} - \overline{\rho}\tilde{u}_j\tilde{c}]}{\partial x_j}\right]\frac{\partial\tilde{c}}{\partial x_i}\frac{\partial\overline{\rho}}{\partial x_i}}_{(T_2)_{res}} + f_{T_2}(Le)\frac{K_c^* S_L}{\delta_{th}(1.0 + Ka_\Delta)^{1/2}}[\overline{\rho}\tilde{N}_c - \overline{\rho}\tilde{D}\nabla\tilde{c}.\nabla\tilde{c}] \tag{9i}$$

$$\text{where } f_{T_2}(Le) = \frac{3.3}{Le^{2.57}erf[4(1.0 - Le) + 1.4]} \text{ and } K_c^* = \frac{\delta_{th}}{S_L}\frac{\int_0^1[\rho N_c\nabla.\vec{u}f_b(c)]_L dc}{\int_0^1[\rho N_c f_b(c)]_L dc} \tag{9ii}$$

In Eq. (9ii) $f_{T_2}(Le)$ accounts for the strengthening of heat release effects with decreasing Le as suggested by the scaling estimate given by Eq. (7i). The parameter K_c^* is a thermo-chemical parameter, which provides information regarding the SDR-weighted dilatation rate $\nabla.\vec{u}$ [34, 36, 65, 66]. The thermo-chemical parameter K_c^* accounts for the correlation between $\nabla.\vec{u}$ and ρN_c within the flame front. It is possible to approximate $f_b(c)$ as $f_b(c) = 1/|\nabla c|_L$ [65, 66], which enables one to evaluate K_c^* from laminar flame data. The thermo-chemical parameter K_c^*/τ is also affected by Le and it is equal to 0.52, 0.67, 0.71, 0.78, and 0.79, respectively, for the $Le = 0.34$, 0.6, 0.8, 1.0, and 1.2 flames considered here. The predictions of Eq. (9) are compared to the predictions of Eq. (8) and T_2 extracted from DNS data in Figure 4, which shows that Eq. (9) satisfactorily predicts the quantitative behavior of T_2 for a range of different values of Δ for flames with Le ranging from 0.34 to 1.2. Eq. (9) becomes exactly equal to Eq. (8) for the $Le = 1.0$ case and thus the predictions of Eqs. (8) and (9) cannot be distinguished from each other for case D in Figure 4.

3.3. Modeling of the scalar turbulence interaction term T_3

The variations of the mean values of T_3 conditional on $\tilde{c}$ are shown in Figure 5 for cases A–E at $\Delta \approx 0.4\delta_{th}$, $1.6\delta_{th}$, and $2.8\delta_{th}$. Figure 5 shows that T_3 assumes predominantly negative values throughout the flame brush for cases A–C, but this term exhibits weak positive values toward both the unburned gas sides of the flame brush before assuming mostly negative values for the major portion of the flame brush in cases D and E. The term T_3 can be expressed as follows [21, 28, 34, 45–48]:

$$T_3 = -\overline{2\rho(e_\alpha\cos^2\alpha + e_\beta\cos^2\beta + e_\gamma\cos^2\gamma)N_c} \tag{10}$$

where e_a, e_β, and e_γ are the most extensive, intermediate, and most compressive principal strain rates and their angles with∇c, respectively. Equation (10) suggests that a predominant collinear alignment of ∇c with e_a (e_γ) leads to a negative (positive) value of T_3. It was discussed elsewhere [21, 28, 34, 45–48]

Downloaded by [Newcastle University] at 06:32 27 July 2016

Downloaded by [Newcastle University] at 06:32 27 July 2016

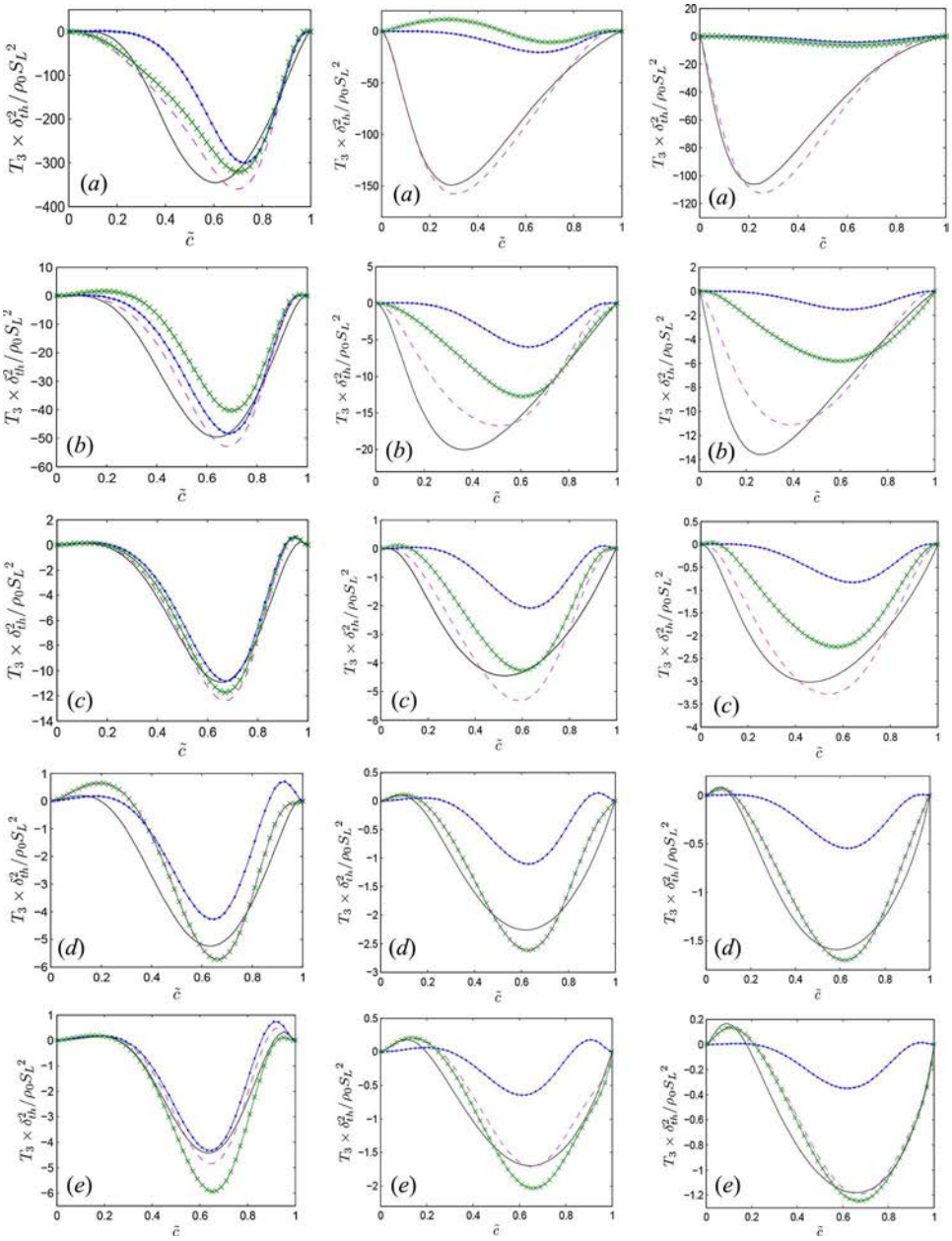

Figure 5. Variations of T_3 (——) and $(T_3)_{res}$ (—●—) conditionally averaged in bins of $\tilde{c}$ along with the predictions of Eqs. (12i) and (12iii) (—×—) and Eqs. (13i) and (13ii) (– – –) for $\Delta \approx 0.4\delta_{th}$ (1st column), $\Delta \approx 1.6\delta_{th}$ (2nd column), and $\Delta \approx 2.8\delta_{th}$ (3rd column) in cases A–E (1st–5th row). All the terms are normalized with respect to $\rho_0 S_L^2/\delta_{th}^2$.

that ∇c predominantly aligns with e_a, when the strain rate induced by the flame normal acceleration overcomes turbulent straining, whereas one obtains preferential alignment of ∇c with e_γ when turbulent straining dominates over the strain rate due to flame normal acceleration. The flame normal acceleration strengthens with decreasing Le, and thus ∇c predominantly aligns with e_a, for the $Le \ll 1$ flames (e.g., cases A and B), leading to negative values of T_3 [21, 22, 28]. By contrast, turbulent straining overcomes the flame normal acceleration on both ends of the flame brush for the $Le \approx 1.0$ cases considered here (e.g., cases C–E), which leads to positive values of T_3 both on unburned and on burned

gas sides of the flame brush for $\Delta \approx 0.4\delta_{th}$. However, the flame normal acceleration dominates over turbulent straining in the middle of the flame brush where the effects of heat release are strong even in the $Le \approx 1.0$ cases considered here (e.g., cases C–E), which leads to negative values of T_3 for the major portion of the flame brush in these cases.

The effects of ∇c alignment with e_a, on T_3 can be scaled in the following manner [28]:

$$T_3 \sim \frac{\rho_0 \tau S_L \tilde{N}_c}{Le^n \delta_{th}} \sim \frac{\rho_0 \tau S_L^2}{Le^{n-1}\delta_{th}^2} \quad \text{where } n > 1 \tag{11i}$$

The contribution of ∇c alignment with e_γ on T_3 can be scaled as follows [28]:

$$T_3 \sim \frac{\rho_0 u'_\Delta \tilde{N}_c}{\Delta} \sim \frac{\rho_0 S_L^2}{\delta_{th}^2} \times Le \times \mathrm{Pr}^{-1/2} \times Ka_\Delta \text{ for } \Delta \gg \delta_{th} \tag{11ii}$$

The Lewis number Le dependence in Eq. (11i) (with $n > 1$) accounts for the greater extent of ∇c alignment with e_a for the flames with $Le << 1.0$. Gao et al. [28] proposed the following scaling estimate of the resolved part of T_3:

$$(T_3)_{res} = -2\bar{\rho}\widetilde{D}\frac{\partial \tilde{c}}{\partial x_i}\frac{\partial \tilde{u}_i}{\partial x_j}\frac{\partial \tilde{c}}{\partial x_j} \sim \frac{\rho_0 S_L^2}{\delta_{th}^2} \times \frac{U_{ref}}{S_L} \times Le^{-1}\ \mathrm{Re}_\Delta^{-1.5} Da_\Delta^{-1.5} \text{ for } \Delta >> \delta_{th} \tag{11iii}$$

A comparison of Eqs. (11i)–(11iii) reveals that the contribution of $(T_3)_{res}$ to T_3 is expected to weaken with increasing Δ, and this behavior can indeed be seen from Figure 5, which shows that the magnitude of $(T_3)_{res}$ decreases with increasing Δ.

Gao et al. [53] utilized the scaling estimates given by Eqs. (11i) and (11ii) to propose a model for T_3 for $Le = 1.0$ flames:

$$T_3 = -2\overline{\rho D}\frac{\partial \tilde{c}}{\partial x_i}\frac{\partial \tilde{u}_i}{\partial x_j}\frac{\partial \tilde{c}}{\partial x_j} + (1 - f_{T_3})(C_3 - C_4 \tau . Da_\Delta^*)\frac{u'_\Delta}{\Delta}\overline{\rho}\tilde{N}_c \tag{12i}$$

where C_3 and C_4 are the model parameters and $Da_L^* = S_L \rho_0 \Delta / u'_\Delta \overline{\rho} \delta_{th}$ is the density-weighted local sub-grid Damköhler number. The symbol f_{T_3} is a bridging function in terms of $\Delta S_L/\alpha_{T0}$, which ensures that $(T_3)_{sg} \approx T_3$ for $\Delta >> \delta_{th}$ and T_3 approaches $(T_3)_{res}$ when the flow is fully resolved:

$$\lim_{\Delta \to 0} T_3 = \lim_{\Delta \to 0}\left(-2\overline{\rho D}\frac{\partial \tilde{c}}{\partial x_i}\frac{\partial \tilde{u}_i}{\partial x_j}\frac{\partial \tilde{c}}{\partial x_j}\right) = -2\rho D\frac{\partial \tilde{c}}{\partial x_i}\frac{\partial \tilde{u}_i}{\partial x_j}\frac{\partial \tilde{c}}{\partial x_j} \tag{12ii}$$

Gao et al. [53] proposed the following expressions for the model parameter C_3, C_4, and f_{T_3}:

$$C_3 = 7.5\,; C_4 = 0.75(1.0 + Ka_\Delta)^{-0.4} \text{ and } f_{T_3} = \exp[-1.05(S_L\Delta/\alpha_{T0})^2] \tag{12iii}$$

It is worth noting that the terms $C_3\overline{\rho}(u'_\Delta/\Delta)\tilde{N}_c$ and $-C_4\rho_0\tau(S_L/\delta_{th})\tilde{N}_c$ are consistent with scaling estimates given by Eqs. (11i) and (11ii), respectively. However, a comparison between Eq. (11i) and $-C_4\rho_0\tau(S_L/\delta_{th})\tilde{N}_c$ reveals that the increased alignment of ∇c with e_α for small values of Le as a result of the strengthening of flame normal acceleration is not accounted for by the model given by Eq. (12ii). The effects of flame normal acceleration are expected to weaken with increasing Karlovitz number as the reacting flow field exhibits some attributes of passive scalar mixing for large values of Karlovitz number in the broken reaction zones regime [55]. This behavior is mimicked here by Ka_Δ dependence of C_4in Eq. (12iii).

The predictions of Eq. (12i) with the model parameters given by Eq. (12ii) are compared to T_3 extracted from DNS data in Figure 5, which shows that Eq. (12i) adequately captures the qualitative and quantitative behaviors of T_3 for the $Le \approx 1.0$ cases considered here (e.g., cases C–E); however, this model has been found to underpredict the magnitude of the negative contribution of T_3 in

Downloaded by [Newcastle University] at 06:32 27 July 2016

the $Le << 1.0$ cases (e.g., cases A and B) for $\Delta > \delta_{th}$. It has already been noted that the increased extent of scalar gradient destruction in the $Le << 1.0$ flames, due to the preferential alignment of ∇c with e_α under strong actions of flame normal acceleration, is not addressed in the model given by Eq. (12i). Thus, this model underpredicts the negative contribution of T_3 for the flames with $Le << 1.0$. Here Eq. (12i) has been modified in the following manner to account for non-unity Lewis number effects:

$$T_3 = -2\overline{\rho D}\frac{\partial \tilde{c}}{\partial x_i}\frac{\partial \tilde{u}_i}{\partial x_j}\frac{\partial \tilde{c}}{\partial x_j} + (1 - f_{T_3})[C_3 - C_4\Gamma(Le)\tau.Da^*_\Delta]\frac{u'_\Delta}{\Delta}\overline{\rho}\tilde{N}_c \tag{13i}$$

$$\text{where} \qquad \Gamma(Le) = \frac{1.7(1-\tilde{c})^p}{Le^{2.57}}\left(\frac{\delta_L}{\delta_{th}}\right)^{1.3} \text{ and } p = 0.2 + 1.5(1.0 - Le) \tag{13ii}$$

The involvement of the function $\Gamma(Le)$ in Eq. (13i) accounts for the strengthening of ∇c alignment with e_α under strong actions of flame normal acceleration in flames with small values of Lewis number. The presence of $(1-\tilde{c})^p$ helps Eq. (13i) capture the qualitative behavior of T_3 across the flame brush. It can be seen from Figure 5 that the model given by Eq. (13i) provides satisfactory qualitative and quantitative predictions of T_3 for all the flames with different values of Le for a range of Δ. It is worth noting that Eq. (13i) approaches Eq. (12i) for $Le = 1.0$ and thus the predictions of Eqs. (12i) and (13i) cannot be distinguished from each other for case D in Figure 5.

3.4. Modeling of the combined reaction, dissipation, and diffusivity gradient contribution [$T_4 - D_2 + f(D)$]

The variations of the mean values of $[T_4 - D_2 + f(D)]$ conditional on $\tilde{c}$ are shown in Figure 6 for A–E for $\Delta \approx 0.4\delta_{th}$, $1.6\delta_{th}$, and $2.8\delta_{th}$. It can be seen from Figure 6 that $[T_4 - D_2 + f(D)]$ acts as a sink (source) term toward the burned (unburned) gas side of the flame brush for $\Delta \approx 0.4\delta_{th}$ and $\Delta \approx 1.6\delta_{th}$; however, the mean value of $[T_4 - D_2 + f(D)]$ conditional on $\tilde{c}$ assumes predominantly negative values for $\Delta \approx 2.8\delta_{th}$. Table 3 shows that the order of magnitudes of T_4, $(-D_2)$, and $f(D)$ remain comparable according to the scaling analysis by Gao et al. [28] and their magnitudes are expected to increase with decreasing Le. Furthermore, the scaling estimates of $(T_4)_{res}$, $(-D_2)_{res}$, and $\{f(D)\}_{res}$ in Table 3 suggest that their contributions are expected to weaken with increasing Δ, where $(T_4)_{res}$, $(-D_2)_{res}$, and $\{f(D)\}_{res}$ are the resolved components of T_4, $(-D_2)$, and $f(D)$, which are given by

$$(T_4)_{res} = 2\tilde{D}\frac{\partial \overline{\dot{w}}}{\partial x_i}\frac{\partial \tilde{c}}{\partial x_i} \tag{14i}$$

$$(-D_2)_{res} = -2\overline{\rho}\tilde{D}^2\frac{\partial^2 \tilde{c}}{\partial x_i \partial x_j}\frac{\partial^2 \tilde{c}}{\partial x_i \partial x_j} \tag{14ii}$$

$$\begin{aligned}\{f(D)\}_{res} = {} & 2\tilde{D}\frac{\partial \tilde{c}}{\partial x_k}\frac{\partial(\overline{\rho}\tilde{D})}{\partial x_k}\frac{\partial^2 \tilde{c}}{\partial x_j \partial x_j} + 2\tilde{D}\frac{\partial \tilde{c}}{\partial x_k}\frac{\partial^2(\overline{\rho}\tilde{D})}{\partial x_j \partial x_k}\frac{\partial \tilde{c}}{\partial x_j} - \frac{\partial}{\partial x_j}\left[\overline{\rho}\tilde{D}\left(\frac{\partial \tilde{c}}{\partial x_k}\frac{\partial \tilde{c}}{\partial x_k}\right)\frac{\partial \tilde{D}}{\partial x_j}\right] \\ & - 2\overline{\rho}\tilde{D}\frac{\partial \tilde{D}}{\partial x_j}\frac{\partial}{\partial x_j}\left(\frac{\partial \tilde{c}}{\partial x_k}\frac{\partial \tilde{c}}{\partial x_k}\right) + \overline{\rho}\left(\frac{\partial \tilde{c}}{\partial x_k}\frac{\partial \tilde{c}}{\partial x_k}\right)\left[\frac{\partial \tilde{D}}{\partial t} + \tilde{u}_j\frac{\partial \tilde{D}}{\partial x_j}\right]\end{aligned} \tag{14iii}$$

Thus, the sub-grid components $(T_4)_{sg} = T_4 - (T_4)_{res}$, $(-D_2)_{sg} = -D_2 + (D_2)_{res}$, and $\{f(D)\}_{sg} = f(D) - \{f(D)\}_{res}$ are expected to play major roles for $\Delta >> \delta_{th}$. The aforementioned behaviors of the resolved and sub-grid components of T_4, $(-D_2)$, and $f(D)$ can be confirmed from Figure 6. It can be seen from Table 3 that the magnitudes of $(T_4)_{sg}$, $(-D_2)_{sg}$, and $\{f(D)\}_{sg}$ remain of the order of $\rho_0 S_L^2/\delta_{th}^2 \sim \overline{\rho}\tilde{N}_c^2$ for $\Delta >> \delta_{th}$; however, their magnitudes are expected to increase with decreasing Le, which can indeed be substantiated from Figure 6.

Downloaded by [Newcastle University] at 06:32 27 July 2016

Downloaded by [Newcastle University] at 06:32 27 July 2016

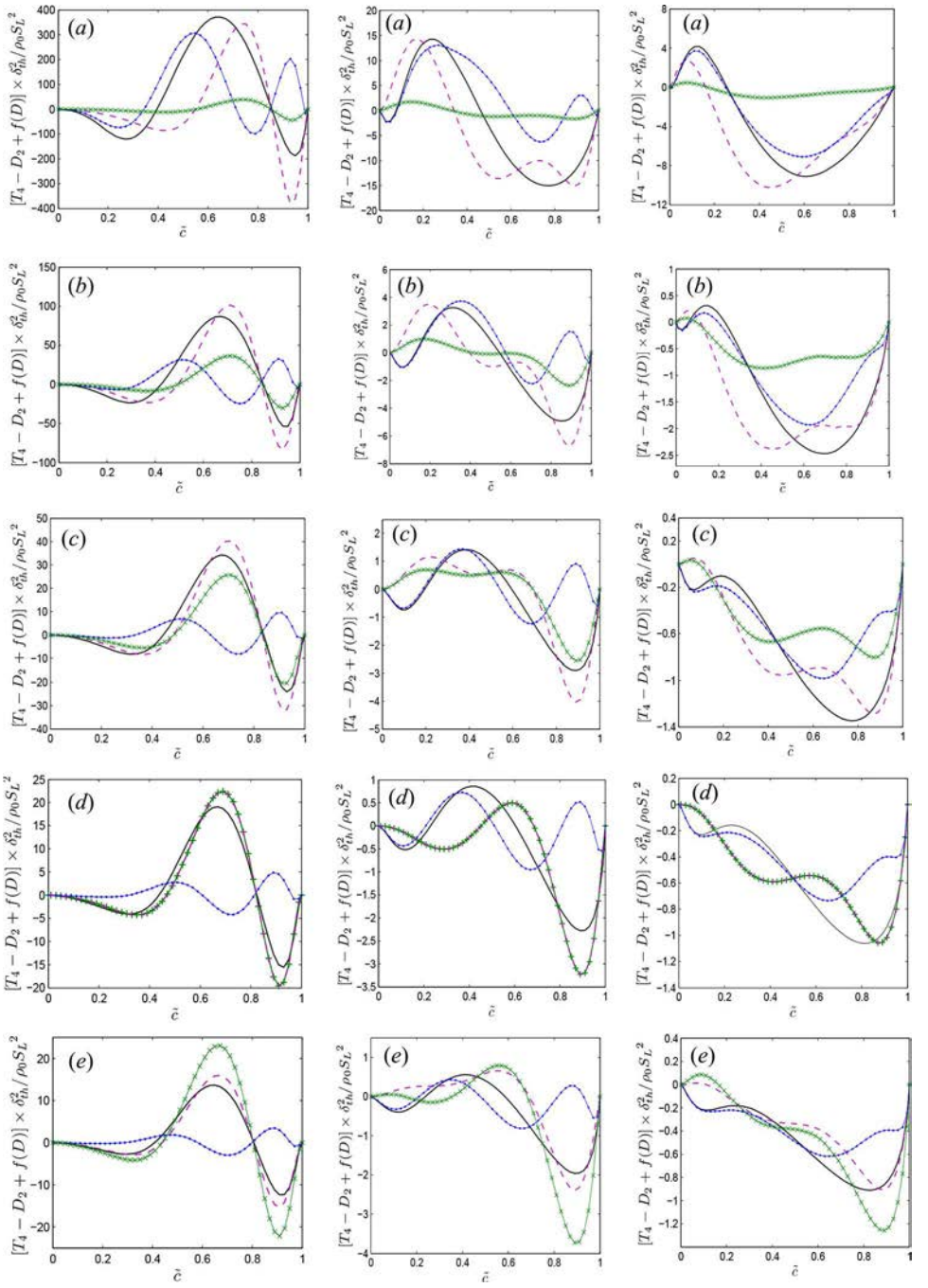

Figure 6. Variations of $[T_4 + f(D) - D_2]$ (——) and $[(T_4)_{sg} - (D_2)_{sg} + \{f(D)\}_{sg}]$ (—●—) conditionally averaged in bins of $\tilde{c}$ along with the predictions of Eqs. (15i) and (15ii) (—×—) and Eq. (16) (– – –) for $\Delta \approx 0.4\delta_{th}$ (1st column), $1.6\delta_{th}$ (2nd column), and $2.8\delta_{th}$ (3rd column) in cases A–E (1st–5th row). All the terms are normalized with respect to $\rho_0 S_L^2/\delta_{th}^2$.

Gao et al. [53] utilized $\{T_4 - D_2 + f(D)\}_{sg} \sim \rho_0 S_L^2/\delta_{th}^2 \sim \overline{\rho}\tilde{N}_c^2$ to model $[T_4 + f(D) - D_2]$ together for unity Lewis number flames by extending an existing RANS model [22, 34, 44, 47, 48, 51] in the following manner:

$$T_4 - D_2 + f(D) = (T_4)_{res} - (D_2)_{res} + \{f(D)\}_{res} - (1 - f_{TD})\beta_3(\tilde{c} - c^*)\overline{\rho}\frac{[\tilde{N}_c - \tilde{D}\nabla\tilde{c}.\nabla\tilde{c}]^2}{\tilde{c}(1-\tilde{c})} \quad (15i)$$

$$\text{where} \quad \beta_3 = 5.7; c^* = 1.0 - 0.83erf\left[0.5\frac{\Delta S_L}{\alpha_{T0}} - 2.3\right] \text{ and } f_{TD} = \exp\left[-0.27\left(\frac{\Delta S_L}{\alpha_{T0}}\right)^{1.7}\right]; \quad (15ii)$$

The involvement of $(\tilde{c} - c^*)/[\tilde{c}(1-\tilde{c})]$ in Eq. (15i) is required for capturing the qualitative behavior of $[T_4 - D_2 + f(D)]$ across the flame brush, whereas f_{TD} approaches unity for small values of Δ as the terms get fully resolved (i.e., $\lim_{\Delta\to 0}[T_4 - D_2 + f(D)] = \lim_{\Delta\to 0}[(T_4)_{res} - (D_2)_{res} + \{f(D)\}_{res}]$). The transition from positive to negative contribution of $[T_4 + f(D) - D_2]$ with increasing Δ has been accounted for by c^*. The predictions of Eq. (15i) are shown in Figure 6, which shows that this model captures both the qualitative and quantitative behaviors of $[T_4 + f(D) - D_2]$ for the $Le \approx 1.0$ cases considered here (e.g., cases C–E); however, this model underpredicts the magnitude of $[T_4 + f(D) - D_2]$ significantly for the $Le \ll 1.0$ cases (e.g., cases A and B). It is worth noting that the model given by Eq. (15i) does not account for the increased magnitude of $\{T_4 - D_2 + f(D)\}_{sg}$ for small values of Le (see Table 3); hence, perhaps it is not surprising that this model under-predicts the magnitude of $[T_4 + f(D) - D_2]$ for the flames with $Le \ll 1.0$ (e.g., cases A and B). The increased magnitude of $[T_4 + f(D) - D_2]$ for the small values of Le is accounted for by modifying Eq. (15i) in the following manner:

$$T_4 - D_2 + f(D) = (T_4)_{res} - (D_2)_{res} + \{f(D)\}_{res} - (1 - f_{TD})\beta'_3(\tilde{c} - c^*)\overline{\rho}\frac{[\tilde{N}_c - \tilde{D}\nabla\tilde{c}.\nabla\tilde{c}]^2}{\tilde{c}(1-\tilde{c})} \quad (16)$$

$$\text{with } \beta'_3 = 5.7\ Le^{-0.2}$$

where c^* and f_{TD} are considered according to Eq. (15ii). The predictions of Eq. (16) are shown in Figure 6, which demonstrates that Eq. (16) captures both the qualitative and quantitative behaviors of $[T_4 + f(D) - D_2]$ for a range of filter widths for different Le cases considered here. Equations (15i) and (16) become equal to each other for $Le = 1.0$ and thus their predictions cannot be separated from each other in case D in Figure 6.

It is worth noting that the combined contribution of the terms D_1, T_4, $f(D)$, and $(-D_2)$ can be expressed in the following manner if the SDR transport equation is derived based on the kinematic form of the progress variable transport equation (i.e., $Dc/Dt = S_d|\nabla c|$) [34, 47]:

$$D_1 + T_4 - D_2 + f(D) \approx -2\overline{D\nabla\cdot(\rho S_d\vec{n}|\nabla c|)|\nabla c|} + 2\overline{D\rho S_d\nabla\cdot\vec{n}|\nabla c|^2} \quad (17)$$

where $S_d = [\dot{w} + \nabla\cdot(\rho D\nabla c)]/(\rho|\nabla c|)$ and $\vec{n} = -\nabla c/|\nabla c|$ are the flame displacement speed and local flame normal vector, respectively. Thus, Eq. (17) suggests that the net contribution of $[T_4 - D_2 + f(D)]$ originates due to flame normal propagation and flame curvature. This justifies the modeling of these terms together [21, 34, 44, 47, 48, 53] because the molecular diffusion term D_1 is a closed term. Although Eq. (16) reasonably captures the qualitative behavior and the magnitude of $[T_4 + f(D) - D_2]$ for all cases considered here, the collective modeling of the terms T_4, $f(D)$, and $(-D_2)$ may give rise to the loss of their individual physical significances. However, this is one of the first attempts to model the Lewis number effects on the SDR transport equation terms in the context of LES of premixed combustion and thus there is a scope for further improvement of this modeling in the future.

3.5. Implications of model implementation

The newly proposed models for the unclosed terms of the SDR $\tilde{N}_c$ transport equation are summarized in Table 4 for the future potential users of these models. It is worth noting that the flamelet assumption is invoked while deriving these models, so they are expected to remain valid in the corrugated flamelets and thin reaction zones regimes of turbulent premixed combustion [55]. The scaling estimates in Table 3 indicate that the terms T_2, T_3, T_4, $(-D_2)$, and $f(D)$ remain leading-order contributors

Downloaded by [Newcastle University] at 06:32 27 July 2016

Table 4. Summary of the proposed models for the unclosed terms of the SDR $\tilde{N}_c$ transport equation (Eq. (3)) in this analysis.

Term	Model expression
$\overline{[\rho u_i N_c - \overline{\rho}\tilde{u}_i\tilde{N}_c]}$	$\overline{[\rho u_i N_c - \overline{\rho}\tilde{u}_i\tilde{N}_c]} = (\Phi-\tilde{c})\frac{\gamma_1\overline{[\rho u_i c - \overline{\rho}\tilde{u}_i\tilde{c}]} - \gamma_2\overline{\rho}\tilde{c}(1-\tilde{c})u'_\Delta M_i}{\tilde{c}(1-\tilde{c})}\tilde{N}_c - \overline{\rho}(C_F\Delta)u'_\Delta\frac{\partial\tilde{N}_c}{\partial x_i}$ where $\gamma_1=1.8$, $\gamma_2=4.9-3.2erf(0.15Re_{t\Delta})$, $Re_{t\Delta}=\rho_0 u'_\Delta\Delta/\mu_0$, $\Phi=0.3(Le-1)+0.7$ and $C_F=0.11$
T_2	$T_2=-\frac{2\tilde{D}}{\overline{\rho}}\left[\overline{\dot{w}}+\frac{\partial}{\partial x_j}\overline{\left(\rho D\frac{\partial c}{\partial x_j}\right)}-\frac{\partial[\overline{\rho u_j c}-\overline{\rho}\tilde{u}_j\tilde{c}]}{\partial x_j}\right]\frac{\partial\tilde{c}}{\partial x_i}\frac{\partial\overline{\rho}}{\partial x_i}+\frac{K_c^* f_{T_2}(Le)S_L}{(1.0+Ka_\Delta)^{1/2}\delta_{th}}[\overline{\rho}\tilde{N}_c-\overline{\rho}\tilde{D}\nabla\tilde{c}.\nabla\tilde{c}]$ where $Ka_\Delta=(u'_\Delta/S_L)^{3/2}(\Delta/\delta_{th})^{-1/2}$ is local sub-grid Karlovitz number and $f_{T_2}(Le)=\frac{3.3}{Le^{2.57}erf[4(1.0-Le)+1.4]}$.
T_3	$T_3=-2\overline{\rho D}\frac{\partial\tilde{c}}{\partial x_i}\frac{\partial\tilde{u}_i}{\partial x_j}\frac{\partial\tilde{c}}{\partial x_j}+(1-f_{T_3})[C_3-C_4\Gamma(Le)\tau.Da^*_\Delta]\frac{u'_\Delta}{\Delta}\overline{\rho}\tilde{N}_c$ where $C_3=7.5$, $C_4=0.75(1.0+Ka_\Delta)^{-0.4}$, $f_{T_3}=\exp[-1.05(\Delta S_L/\alpha_{T0})^2]$ and $Da^*_L=S_L\rho_0\Delta/u'_\Delta\overline{\rho}\delta_{th}$ $\Gamma(Le)=\frac{1.7(1-\tilde{c})^p}{Le^{2.57}}\left(\frac{\delta_L}{\delta_{th}}\right)^{1.3}$ with $p=0.2+1.5(1-Le)$
$[T_4-D_2+f(D)]$	$T_4-D_2+f(D)=(T_4)_{res}-(D_2)_{res}+\{f(D)\}_{res}-(1-f_{TD})\beta'_3\overline{\rho}(\tilde{c}-c*)\frac{[\tilde{N}_c-\tilde{D}\nabla\tilde{c}.\nabla\tilde{c}]^2}{\tilde{c}(1-\tilde{c})}$ where $(T_4)_{res}=2\tilde{D}\frac{\partial\overline{\dot{w}}}{\partial x_i}\frac{\partial\tilde{c}}{\partial x_i}$, $(-D_2)_{res}=-2\overline{\rho}\tilde{D}^2\frac{\partial^2\tilde{c}}{\partial x_i\partial x_j}\frac{\partial^2\tilde{c}}{\partial x_i\partial x_j}$, $\{f(D)\}_{res}=2\tilde{D}\frac{\partial\tilde{c}}{\partial x_k}\frac{\partial(\overline{\rho}\tilde{D})}{\partial x_k}\frac{\partial^2\tilde{c}}{\partial x_j\partial x_j}+2\tilde{D}\frac{\partial\tilde{c}}{\partial x_k}\frac{\partial^2(\overline{\rho}\tilde{D})}{\partial x_j\partial x_k}\frac{\partial\tilde{c}}{\partial x_j}-\frac{\partial}{\partial x_j}\left[\overline{\rho}\tilde{D}\nabla\tilde{c}.\nabla\tilde{c}\frac{\partial\tilde{D}}{\partial x_j}\right]$, $-2\overline{\rho}\tilde{D}\frac{\partial\tilde{D}}{\partial x_j}\frac{\partial(\nabla\tilde{c}.\nabla\tilde{c})}{\partial x_j}+\overline{\rho}\nabla\tilde{c}.\nabla\tilde{c}\left[\frac{\partial\tilde{D}}{\partial t}+\tilde{u}_j\frac{\partial\tilde{D}}{\partial x_j}\right]$, $f_{TD}=\exp[-0.27(S_L\Delta/\alpha_{T0})^{1.7}]$, $c*=1.0-0.83erf[0.5(\Delta S_L/\alpha_{t0})-2.3]$ and $\beta'_3=5.7/Le^{0.2}$

to the SDR $\tilde{N}_c$ transport and the magnitude of T_1 remains negligible compared with the terms T_2, T_3, T_4, $(-D_2)$, and $f(D)$ irrespective of Damköhler and turbulent Reynolds numbers. This is consistent with the observations made from Figure 2. However, the turbulent transport term T_1 still needs to be modeled and included in the model implementation for LES for numerical stability.

4. Conclusions

The effects of global Lewis number *Le* on the modeling of the unclosed terms of the transport equation of Favre-filtered SDR $\tilde{N}_c$ have been analyzed based on *a priori* analysis of a DNS database of freely propagating statistically planar turbulent premixed flames with *Le* ranging from 0.34 to 1.2. It has been found that *Le* has profound influence on the statistical behavior of the unclosed terms of $\tilde{N}_c$ transport arising from turbulent transport T_1, density variation due to heat release T_2, alignment of scalar and velocity gradients T_3, correlation between the gradients of reaction rate and reaction progress variable T_4, molecular dissipation $(-D_2)$, and diffusivity gradients $f(D)$, and detailed physical explanations have been provided for the observed non-unity Lewis number effects. Recently proposed models for T_1, T_2, T_3, T_4, $(-D_2)$, and $f(D)$ for unity Lewis number flames have been extended here to account for the effects of *Le* based on the scaling estimates of these unclosed terms [28]. The newly proposed models have been found to satisfactorily predict the unclosed terms obtained from explicitly filtered DNS data for a range of Δ for different values of *Le*. However, it is still essential to implement these models into actual LES simulations for the purpose of *a posteriori* assessment. Moreover, these models need to be further validated based on detailed chemistry-based DNS simulations. Further validation of these models will form the basis of future investigations.

Downloaded by [Newcastle University] at 06:32 27 July 2016

Funding

The financial assistance of the Engineering and Physical Science (EPSRC) research council of the UK (EP/I028013/1) and computational support of N8 are gratefully acknowledged.

References

[1] Y. Huang and V. Yang, Dynamics and Stability of Lean-Premixed Swirl Stabilised Combustion, *Prog. Energy Combust. Sci*., vol. 35, no. 4, pp. 293–364, 2009.
[2] T. Wallner, H. K. Ng, and R. W. Peters, The Effects of Blending Hydrogen with Methane on Energy Operation, Efficiency and Emissions, *Proc. SAE Trans*., 2007–01-0474, 2007.
[3] R. Schefer, Reduced Turbine Emissions Using Hydrogen-Enriched Fuels, Proc. of the 2002 U.S. DOE Hydrogen Program Review NREL/CP-610–32405, 2002.
[4] M. Mizomoto, S. Asaka, S. Ikai, and C. K. Law, Effects of Preferential Diffusion on the Burning Intensity of Curved Flames, *Proc. Combust. Inst*., vol. 20, pp. 1933–1939, 1984.
[5] C. K. Law and O. C. Kwon, Effects of Hydrocarbon Substitution on Atmospheric Hydrogen–Air Flame Propagation, *Int. J. Hydrogen Energy*, vol. 29, pp. 867–879, 2004.
[6] F. Dinkelacker, B. Manickam, and S. R. Mupppala, Modelling and Simulation of Lean Premixed Turbulent Methane/Hydrogen/Air Flames with an Effective Lewis Number Approach, *Combust. Flame*, vol. 158, pp. 1742–1749, 2011.
[7] P. Pelce and P. Clavin, Influence of Hydrodynamics and Diffusion Upon the Stability Limits of Laminar Premixed Flames, *J. Fluid Mech*., vol. 124, pp. 219–237, 1982.
[8] P. Clavin and F. A. Williams, Effects of Molecular Diffusion and Thermal Expansion on the Structure and Dynamics of Turbulent Premixed Flames in Turbulent Flows of Large Scale and Small Intensity, *J. Fluid Mech*., vol. 128, pp. 251–282, 1982.
[9] P. A. Libby, A. Linan, and F. A. Williams, Strained Premixed Laminar Flames with Non-Unity Lewis Numbers, *Combust. Sci. Technol*., vol. 34, pp. 257–293, 1983.
[10] G. I. Sivashinsky, Instabilities, Pattern Formation and Turbulence in Flames, *Annu. Rev. Fluid Mech*., vol. 15, pp. 179–190, 1983.
[11] R. G. Abdel-Gayed, D. Bradley, M. Hamid, and M. Lawes, Lewis Number Effects on Turbulent Burning Velocity, *Proc. Combust. Inst*., vol. 20, pp. 505–512, 1984.
[12] W. T. Ashurst, N. Peters, and M. D. Smooke, Numerical Simulation of Turbulent Flame Structure with Non-Unity Lewis Number, *Combust. Sci. Technol*., vol. 53, pp. 339–375, 1987.
[13] D. Haworth and T. J. Poinsot, Numerical Simulations of Lewis Number Effects in Turbulent Premixed Flames, *J. Fluid Mech*., vol. 244, pp. 405–436, 1992.
[14] C. J. Rutland and A. Trouvé, Direct Simulations of Premixed Turbulent Flames with Nonunity Lewis Numbers, *Combust. Flame*, vol. 94, pp. 41–57, 1993.
[15] A. Trouvé and T. J. Poinsot, The Evolution Equation for Flame Surface Density in Turbulent Premixed Combustion, *J. Fluid Mech*., vol. 278, pp. 1–31, 1994.
[16] N. Chakraborty, and R. S. Cant, Influence of Lewis Number on Curvature Effects in Turbulent Premixed Flame Propagation in the Thin Reaction Zones Regime, *Phys. Fluids*, vol. 17, 105105, 2005.
[17] J. Yuan, Y. Ju, and C. K. Law, Coupled Hydrodynamic, and Diffusional Thermal Instabilities in Flame Propagation at Small Lewis Numbers, *Phys. Fluids*, vol. 17, 074106, 2005.
[18] N. Chakraborty and M. Klein, A Priori Direct Numerical Simulation Assessment of Algebraic Flame Surface Density Models for Turbulent Premixed Flames in the Context of Large Eddy Simulation. *Phys. Fluids*, vol. 20, 085108, 2008.
[19] I. Han and K. H. Huh, Roles of Displacement Speed on Evolution of Flame Surface Density for Different Turbulent Intensities and Lewis Numbers in Turbulent Premixed Combustion, *Combust. Flame*, vol. 152, pp. 194–205, 2008.
[20] N. Chakraborty, and R. S. Cant, Effects of Lewis Number on Scalar Transport in Turbulent Premixed Flames, *Phys. Fluids*, vol. 21, 035110, 2009.
[21] N. Chakraborty, M. Klein, and N. Swaminathan, Effects of Lewis Number on Reactive Scalar Gradient Alignment with Local Strain Rate in Turbulent Premixed Flames, *Proc. Combust. Inst*., vol. 32, pp. 1409–1417, 2009.
[22] N. Chakraborty and N. Swaminathan, Effects of Lewis Number on Scalar Dissipation Transport and Its Modelling Implications for Turbulent Premixed Combustion, *Combust. Sci. Technol*., vol. 182, pp. 1201–1240, 2010.
[23] N. Chakraborty and R. S. Cant, Effects of Lewis Number on Flame Surface Density Transport in Turbulent Premixed Combustion, *Combust. Flame*, vol. 158, pp. 1768–1787, 2011.
[24] N. Chakraborty, M. Katragadda, and R. S. Cant, Effects of Lewis Number on Turbulent Kinetic Energy Transport in Turbulent Premixed Combustion, *Phys. Fluids*, vol. 23, 075109, 2011.
[25] N. Chakraborty, and N. Swaminathan, Effects of Lewis Number on Scalar Variance Transport in Turbulent Premixed Flames, *Flow, Turb. Combust*., vol. 87, nos. 2–3, pp. 261–292, 2011.

Downloaded by [Newcastle University] at 06:32 27 July 2016

[26] N. Chakraborty, and A. N. Lipatnikov, Effects of Lewis Number on the Statistics of Conditional Fluid Velocity in Turbulent Premixed Combustion in the Context of Reynolds Averaged Navier Stokes Simulations, *Phys. Fluids*, vol. 25, 045101, 2013.
[27] N. Chakraborty, L. Wang, and M. Klein, Effects of Lewis Number on Streamline Segment Analysis of Turbulent Premixed Flames, *Phys. Rev. E*, vol. 89, 033015, 2014.
[28] Y. Gao, N. Chakraborty, and N. Swaminathan, Scalar Dissipation Rate Transport in the Context of Large Eddy Simulations for Turbulent Premixed Flames with Non-Unity Lewis Number, *Flow Turb. Combust*., vol. 93, pp. 461–486, 2014.
[29] R. W. Bilger, Some Aspects of Scalar Dissipation, *Flow Turb. Combust*., vol. 72, pp. 93–114, 2004.
[30] R. O. Fox, Computational Models for Turbulent Reacting Flow, Cambridge University Press, Cambridge, UK, 2003.
[31] N. Kasagi, Y. Tomita, and A. Kuroda, Direct Numerical Simulation of Passive Scalar Field in a Turbulent Channel Flow, *J. Heat Transfer*, vol. 114, no. 3, pp. 598–606, 2008.
[32] S. C. P. Cheung, G. H. Yeoh, A. L. K. Cheung, R. K. K. Yuen, and S. M. Lo, Flickering Behaviour of Turbulent Fires Using Large Eddy Simulation, *Numer. Heat Trans. A*., vol. 52, no. 7, pp. 679–712, 2007.
[33] K. N. C. Bray, Turbulent Flows with Premixed Reactants, in P. A. Libby, and F. A. Williams, (eds.), *Turbulent Reacting Flows*, Springer Verlag, Berlin Heidelburg, New York, pp. 115–183, 1980.
[34] N. Chakraborty M. Champion A. Mura, and N. Swaminathan, Scalar Dissipation Rate Approach to Reaction Rate Closure, in N. Swaminathan, and K. N. C. Bray, (eds.), *Turbulent Premixed Flame*, 1st ed., Cambridge University Press, Cambridge, UK, pp. 76–1023, 2011.
[35] S. P. Malkeson and N. Chakraborty, The Modeling of Fuel Mass Fraction Variance Transport in Turbulent Stratified Flames: A Direct Numerical Simulation Study, *Numer. Heat Trans. A*., vol. 58, no. 3, pp. 187–206, 2010.
[36] T. Dunstan, Y. Minamoto, N. Chakraborty, and N. Swaminathan, Scalar Dissipation Rate Modelling for Large Eddy Simulation of Turbulent Premixed Flames, *Proc. Combust. Inst*., vol. 34, pp. 1193–1201, 2013.
[37] Y. Gao, N. Chakraborty, and N. Swaminathan, Algebraic Closure of Scalar Dissipation Rate for Large Eddy Simulations of Turbulent Premixed Combustion, *Combust. Sci. Technol*., vol. 186, pp. 1309–1337, 2014.
[38] T. Ma, Y. Gao, A. M. Kempf, and N. Chakraborty, Validation and Implementation of Algebraic LES Modelling of Scalar Dissipation Rate for Reaction Rate Closure in Turbulent Premixed Combustion, *Combust. Flame*, vol. 161, pp. 3134–3153, 2014.
[39] M. S. Raju, Application of Scalar Monte-Carlo Probability Density Function Method for Turbulent Spray Flames, *Numer. Heat Trans. A*, vol. 30, no. 8, pp. 753–777, 1996.
[40] Y. Pei, E. R. Hawkes, and S. Kook, Transported Probability Density Function Modelling of the Vapour Phase of an n-Heptane Jet at Diesel Engine Conditions, *Proc. Combust. Inst*., vol. 34, pp. 3039–3047, 2013.
[41] Y. Pei, E. R. Hawkes, and S. Kook, A Comprehensive Study of Effects of Mixing, and Chemical Kinetic Models on Predictions of n-Heptane Jet Ignitions with the PDF Method, *Flow, Turb. Combust*., vol. 91, pp. 249–280, 2013.
[42] T. Mantel and R. Borghi, New Model of Premixed Wrinkled Flame Propagation Based on a Scalar Dissipation Equation, *Combust. Flame*, vol. 96, no. 4, pp. 443–457, 1994.
[43] A. Mura and R. Borghi, Towards an Extended Scalar Dissipation Equation for Turbulent Premixed Combustion, *Combust. Flame*, vol. 133, pp. 193–196, 2003.
[44] N. Swaminathan and K. N. C. Bray, Effect of Dilatation on Scalar Dissipation in Turbulent Premixed Flames, *Combust. Flame*, vol. 143, pp. 549–565, 2005.
[45] N. Chakraborty, and N. Swaminathan, Influence of Damköhler Number on Turbulence-Scalar Interaction in Premixed Flames, Part I: Physical Insight, *Phys. Fluids*, vol. 19, 045103, 2007.
[46] N. Chakraborty, and N. Swaminathan, Influence of Damköhler Number on Turbulence-Scalar Interaction in Premixed Flames, Part II: Model Development, *Phys. Fluids*, vol. 19, 045104, 2007.
[47] N. Chakraborty, J. W. Rogerson, and N. Swaminathan, *A Priori* Assessment of Closures for Scalar Dissipation Rate Transport in Turbulent Premixed Flames Using Direct Numerical Simulation, *Phys. Fluids*, vol. 20, 045106, 2008.
[48] N. Chakraborty, J. W. Rogerson, and N. Swaminathan, The Scalar Gradient Alignment Statistics of Flame Kernels and Its Modelling Implications for Turbulent Premixed Combustion, *Flow Turb. Combust*., vol. 85, pp. 25–55, 2010.
[49] A. Mura, K. Tsuboi, and T. Hasegawa, Modelling of the Correlation between Velocity and Reactive Scalar Gradients in Turbulent Premixed Flames based on DNS Data. *Combust. Theor. Modell*., vol. 12, pp. 671–698, 2008.
[50] A. Mura, V. Robin, M. Champion, and T. Hasegawa, Small-Scale Features of Velocity and Scalar Fields of Turbulent Premixed Flames, *Flow Turb. Combust*., vol. 82, pp. 339–358, 2009.
[51] N. Chakraborty and N. Swaminathan, Effects of Turbulent Reynolds Number on the Scalar Dissipation Rate Transport in Turbulent Premixed Flames in the Context of Reynolds Averaged Navier Stokes Simulations, *Combust. Sci. Technol*., vol. 185, pp. 676–709, 2013.
[52] E. Knudsen, E. S. Richardson, E. M. Doran, H. Pitsch, and J. H. Chen, Modeling Scalar Dissipation, and Scalar Variance in Large Eddy Simulation: Algebraic, and Transport Equation Closures, *Phys. Fluids*, vol. 24, 055103, 2012.
[53] Y. Gao, N. Chakraborty, and N. Swaminathan, Scalar Dissipation Rate Transport and Its Modelling for Large Eddy Simulations of Turbulent Premixed Combustion, *Combust. Sci. Technol*., vol. 187, no. 3, pp. 362–383, 2015.

Downloaded by [Newcastle University] at 06:32 27 July 2016

[54] J. H. Chen, A. Choudhary, D. De Supinski, E. R. Hawkes, S. Klasky, W. K. Liao, K. L. Ma, J. Mellor-Crummey, N. Podhorski, R. Sankaran, S. Shende, and C. S. Yoo, Terascale Direct Numerical Simulations of Turbulent Combustion using S3D, *Comput. Sci. Discov.*, vol. 2, no. 1, 015001, 2009.
[55] N. Peters, *Turbulent Combustion*, Cambridge University Press, Cambridge, UK, 2000.
[56] K. W. Jenkins and R. S. Cant, DNS of Turbulent Flame Kernels, in C. Liu, L. Sakell, and T. Beautner, (eds.), *Proc. Second AFOSR Conf. on DNS and LES*, Kluwer Academic Publishers, New Brunswick, NJ, pp. 191–202, 1999.
[57] M. Boger, D. Veynante, H. Boughanem, and A. Trouvé, Direct Numerical Simulation Analysis of Flame Surface Density Concept for Large Eddy Simulation of Turbulent Premixed Combustion, *Proc. Combust. Inst.*, vol. 27, pp. 917–925, 1998.
[58] F. Charlette, C. Meneveau, and D. Veynante, A Power-Law Flame Wrinkling Model for LES of Premixed Turbulent Combustion. Part I: Non-Dynamic Formulation and Initial Tests, *Combust. Flame*, vol. 131, pp. 159–180, 2002.
[59] R. W. Grout, An Age-Extended Progress Variable for Conditioning Reaction Rates, *Phys. Fluids*, vol. 19, 105107, 2007.
[60] H. Reddy, and J. Abraham, Two-Dimensional Direct Numerical Simulation Evaluation of the Flame Surface Density Model for Flames Developing from an Ignition Kernel in Lean Methane/Air Mixtures Under Engine Conditions, *Phys. Fluids*, vol. 24, 105108, 2012.
[61] C. Pera, S. Chevillard, and J. Reveillon, Effects of Residual Burnt Gas Heterogeneity on Early Flame Propagation and on Cyclic Variability in Spark-Ignited Engines, *Combust. Flame*, vol. 160, pp. 1020–1032, 2013.
[62] D. Veynante, A. Trouvé, K. N. C. Bray, and T. Mantel, Gradient and Countergradient Turbulent Scalar Transport in Turbulent Premixed Flames, *J. Fluid Mech.*, vol. 332, pp. 263–293, 1997.
[63] N. Chakraborty and R. S. Cant, Effects of Turbulent Reynolds Number on Turbulent Scalar Flux Modelling in Premixed Flames using Reynolds Averaged Navier-Stokes Simulations, *Numer. Heat Trans. A*, vol. 67, no. 11, pp. 1187–1207, 2015.
[64] Y. Gao, N. Chakraborty, and M. Klein, Assessment of the Performances of Sub-Grid Scalar Flux Models for Premixed Flames with Different Global Lewis Numbers: A Direct Numerical Simulation Analysis, *Int. J. Heat Fluid Flow*, vol. 52, pp. 28–39, 2015.
[65] H. Kolla, J. Rogerson, N. Chakraborty, and N. Swaminathan, Prediction of Turbulent Flame Speed using Scalar Dissipation Rate, *Combust. Sci. Technol.*, vol. 181, pp. 518–535, 2009.
[66] J. W. Rogerson and N. Swaminathan, Correlation between Dilatation and Scalar Dissipation in Turbulent Premixed Flames, Proc. 3rd European Combustion Meeting Crete, China, Greece, 11th to 13th April, 2007.

Downloaded by [Newcastle University] at 06:32 27 July 2016